Bacterial esterases reverse lipopolysaccharide ubiquitylation to block host immunity

Szczesna, M.; Huang, Y.Z.; Lacoursiere, R.E.; Bonini, F.; Pol, V.; Koc, F.; ... ; Thurston, T.L.M.

Article

Cell Host & Microbe

Bacterial esterases reverse lipopolysaccharide ubiquitylation to block host immunity

Graphical abstract

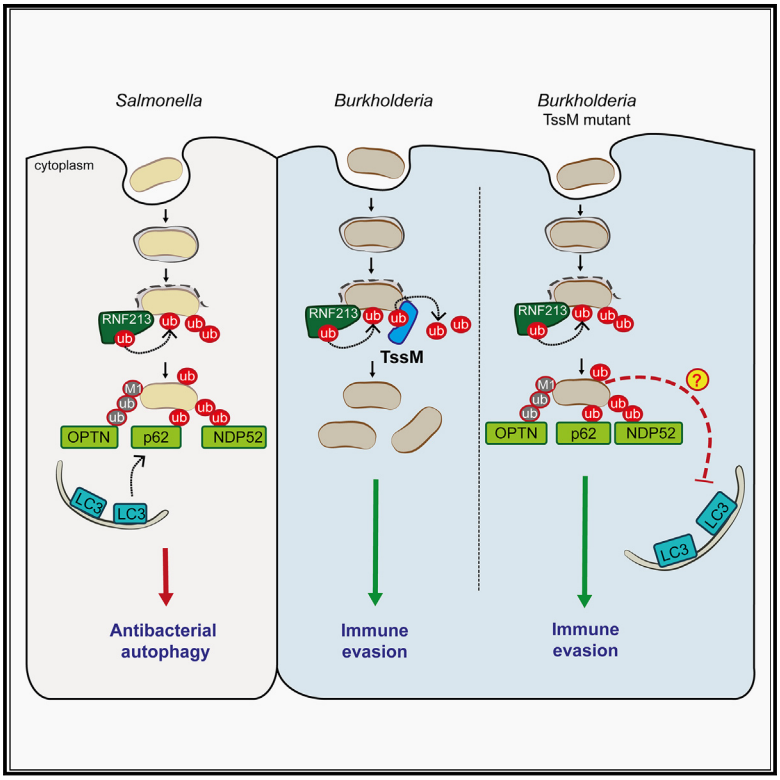

Authors

Magdalena Szczesna, Yizhou Huang, Rachel E. Lacoursiere, ..., Paul P. Geurink, Jonathan N. Pruneda, Teresa L.M. Thurston

Correspondence

pruneda@ohsu.edu (J.N.P.), t.thurston@imperial.ac.uk (T.L.M.T.)

In brief

Szczesna et al. identify a virulence mechanism used by intracellular bacterial pathogens to evade cell-autonomous immune defenses. A secreted effector removes ubiquitin earmarks deposited by the host E3 ligase RNF213 as part of a larger strategy to prevent bacterial recognition and destruction.

Highlights

- *Burkholderia* reverse bacterial LPS ubiquitylation with the ubiquitin esterase TssM
- Additional *Burkholderia* factors redundantly block antibacterial autophagy
- A structure of TssM guides design of a variant with high esterase specificity
- TssM belongs to a family of ubiquitin esterases encoded by intracellular pathogens

Szczesna et al., 2024, Cell Host & Microbe *32*, 913–924
June 12, 2024
https://doi.org/10.1016/j.chom.2024.04.012

CellPress

Cell Host & Microbe

CellPress
OPEN ACCESS

Article

Bacterial esterases reverse lipopolysaccharide ubiquitylation to block host immunity

Magdalena Szczesna,[1] Yizhou Huang,[1,4] Rachel E. Lacoursiere,[2,4] Francesca Bonini,[1] Vito Pol,[3] Fulya Koc,[1] Beatrice Ward,[1] Paul P. Geurink,[3] Jonathan N. Pruneda,[2,*] and Teresa L.M. Thurston[1,5,*]

[1]Department of Infectious Disease, Centre for Bacterial Resistance Biology, Imperial College London, London SW7 2AZ, UK
[2]Department of Molecular Microbiology & Immunology, Oregon Health & Science University, Portland, OR 97239, USA
[3]Department of Cell and Chemical Biology, Leiden University Medical Centre, Leiden, the Netherlands
[4]These authors contributed equally
[5]Lead contact
*Correspondence: pruneda@ohsu.edu (J.N.P.), t.thurston@imperial.ac.uk (T.L.M.T.)
https://doi.org/10.1016/j.chom.2024.04.012

SUMMARY

Aspects of how *Burkholderia* escape the host's intrinsic immune response to replicate in the cell cytosol remain enigmatic. Here, we show that *Burkholderia* has evolved two mechanisms to block the activity of Ring finger protein 213 (RNF213)-mediated non-canonical ubiquitylation of bacterial lipopolysaccharide (LPS), thereby preventing the initiation of antibacterial autophagy. First, *Burkholderia's* polysaccharide capsule blocks RNF213 association with bacteria and second, the *Burkholderia* deubiquitylase (DUB), TssM, directly reverses the activity of RNF213 through a previously unrecognized esterase activity. Structural analysis provides insight into the molecular basis of TssM esterase activity, allowing it to be uncoupled from its isopeptidase function. Furthermore, a putative TssM homolog also displays esterase activity and removes ubiquitin from LPS, establishing this as a virulence mechanism. Of note, we also find that additional immune-evasion mechanisms exist, revealing that overcoming this arm of the host's immune response is critical to the pathogen.

INTRODUCTION

Pathogenic bacteria have evolved diverse mechanisms to counteract cell-autonomous immunity, which otherwise guards both immune and non-immune cells from the onset of an infection.[1,2] Ring finger protein 213 (RNF213) has recently emerged as a versatile immune sensor, restricting the growth of Gram-negative and Gram-positive bacteria as well as parasites and viruses.[3–6] The protein represents a large and unusual E3 ligase[7] that mediates the direct and non-canonical ester-linked ubiquitylation of lipopolysaccharide (LPS), marking bacteria that sporadically enter the cytosol for destruction by antibacterial autophagy.[5]

Burkholderia pseudomallei (Bp) is a Gram-negative bacterium endemic in large parts of the tropics that causes melioidosis, a disease associated with high rates of fatalities in humans.[8] Species related to *B. pseudomallei*, including *B. mallei* and *B. thailandensis* (Bt), replicate freely in the host cell cytosol of both non-phagocytic and phagocytic immune cells.[9]

Their intracellular growth and ability to survive inside the host rely on key virulence proteins implicated in phagosomal escape, cell to cell spread, or inhibition of innate immune signaling.[10] Yet, despite indications that *Burkholderia* evade antibacterial autophagy,[11,12] it remains to be determined whether, and how, cytosolic bacteria, including *Burkholderia* spp., evade restriction by the recently identified immune sensor, RNF213. In this study, we identify ubiquitylated LPS as a substrate for the *Burkholderia* deubiquitylase (DUB) TssM and demonstrate that TssM is a potent esterase that reverses the activity of host immune sensor RNF213.

RESULTS

RNF213 senses intracellular *Burkholderia*

Immunofluorescence microscopy showed that *B. thailandensis* strain E264 became coated with the immune sensor RNF213 (Figure 1A). The percentage of RNF213-coated E264 bacteria accumulated over time, reaching more than 80% at 6 h post invasion (Figure 1B). Up to 30% of a second *B. thailandensis* strain, E555, containing a polysaccharide capsule like that of *B. pseudomallei*,[13,14] was also coated with RNF213 (Figure 1B). Despite RNF213 recruitment to *B. thailandensis*, less than 10% of either strain accumulated a ubiquitin coat, even at 6 h post invasion (Figures 1A and 1B). To further investigate this potential *Burkholderia*-mediated block in RNF213 activity, we analyzed the ubiquitylation of cytosolic bacteria by immunoblot. In agreement with previous findings,[5] bacteria isolated from cells infected with wildtype (WT) *Salmonella* yielded a high molecular weight, ubiquitin-positive smear that was absent in non-infected cells and dependent on RNF213 (Figure 1C). The semi-rough LPS mutant *Salmonella* strain (Δ*rfc*), containing just one O-antigen unit, had a distinct, ubiquitin-positive banding pattern of lower molecular mass, indicating that LPS is the target of

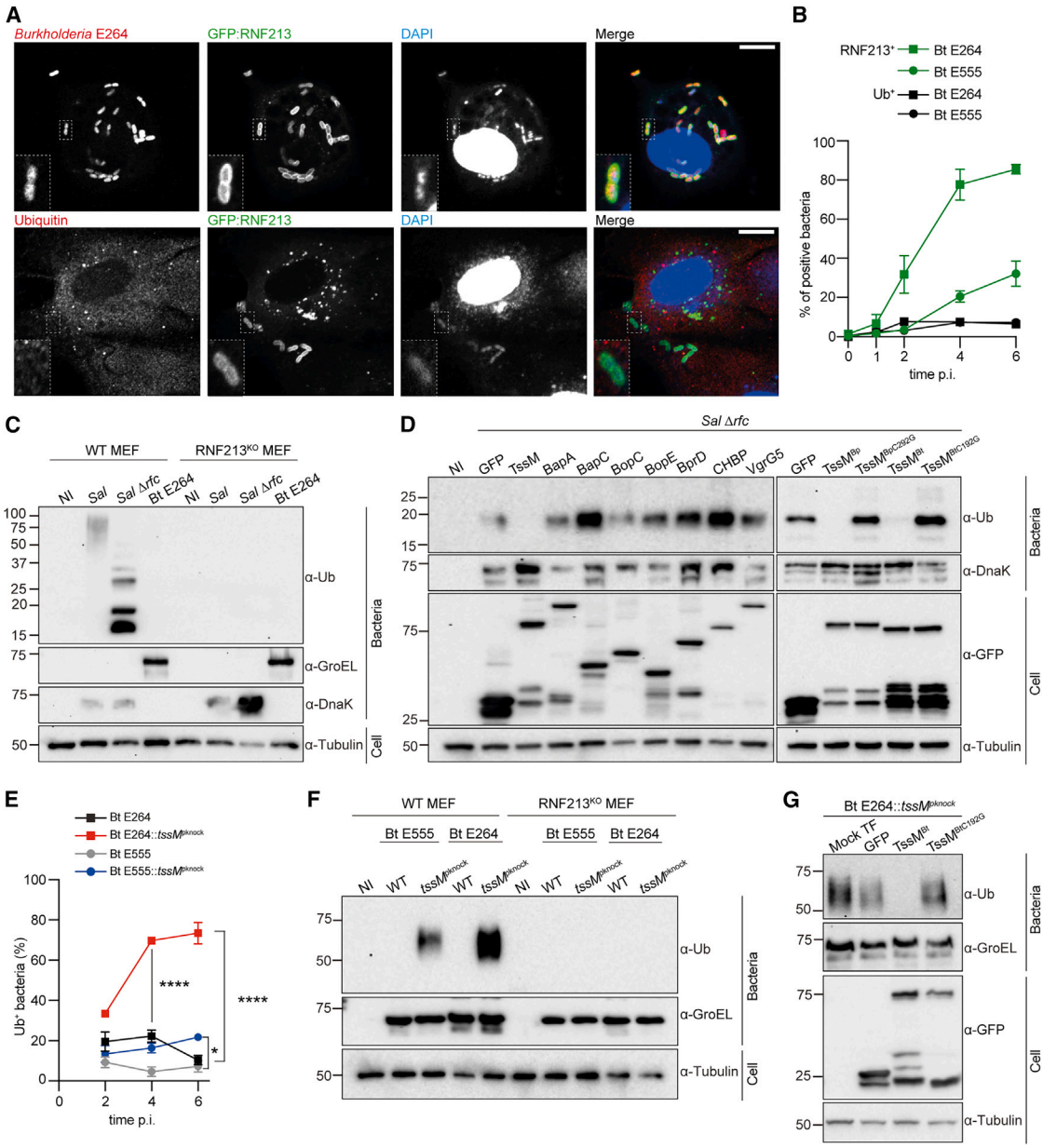

Figure 1. *Burkholderia* effector TssM counteracts the activity of RNF213

(A) Representative confocal microscopy images of RNF213-knockout (RNF213^{KO}) mouse embryonic fibroblasts (MEFs)[5] stably expressing GFP-RNF213, infected with *B. thailandensis* E264 (bottom panel) or E264 pH4-GroS-RFP (top panel) and fixed at 6 h post invasion (p.i.). Samples were labeled with an anti-ubiquitin (Ub) antibody when indicated. Scale bar = 10 μm.

(B) Immunofluorescence-based quantification of marker-positive *B. thailandensis* E264 and E555 strains in RNF213^{KO} MEFs stably expressing GFP-RNF213. Ub localization was quantified following infection of WT MEFs and immunolabelling.

(C) Immunoblots of indicated *Salmonella* (*Sal*) and *B. thailandensis* (Bt) strains isolated from infected MEFs at 4 h or 24 h p.i., respectively, or non-infected (NI) cells as a control. Cell lysates and isolated intracellular bacteria were immunoblotted with the indicated antibodies. DnaK and GroEL were used as loading controls for *Salmonella* and *Burkholderia*, respectively.

(D) Immunoblot analysis of Δ*rfc Salmonella* strain isolated from infected HEK293ET cells that were transiently transfected with plasmids encoding the indicated N-terminal GFP-tagged effector from *B. pseudomallei* or *B. thailandensis*. Cell lysates and isolated intracellular bacteria were immunoblotted with the indicated antibodies.

(E) Immunofluorescence-based quantification of the percentage of Ub-coated bacteria over time in WT MEFs infected with indicated *B. thailandensis* strains.

(F) Immunoblot analysis of indicated *B. thailandensis* strains isolated from infected WT or RNF213^{KO} MEFs at 24 h p.i.

(G) Immunoblot analysis of HEK293ET cells transiently transfected with plasmids encoding the indicated GFP-tagged effector and infected with the Bt E264::*tssM*^{pknock} strain. Mock transfected cells (mock TF), refers to cells that did not receive DNA. Values show mean of three biological repeats ± SEM (B and E). Other data are representative of at least three biological repeats. Statistical significance was assessed by two-way ANOVA with Sidak's multiple comparisons test (E); **** <0.0001.

See also Figure S1.

RNF213-mediated ubiquitylation.[5] However, no ubiquitin smear was detected with *B. thailandensis* obtained from infected WT or RNF213^{KO} cells (Figure 1C). Therefore, RNF213 detects intracellular *B. thailandensis*, but the evident lack of associated ubiquitylation strongly suggests that *Burkholderia* evades, inhibits, or reverses the activity of RNF213.

Burkholderia TssM counters RNF213

We hypothesized that a secreted *Burkholderia* virulence protein (effector) counteracts the activity of RNF213. To test this, we exploited the RNF213-mediated ubiquitylation of Δ*rfc Salmonella* and exogenously expressed eight previously defined and verified *B. pseudomallei* secreted effectors[15,16] to search, *in trans*, for anti-RNF213 activity. Following infection of cells expressing GFP or the following N-terminally GFP-tagged effectors; BapA, BapC, BopC, BopE, BprD, CHBP, or VgrG5, Δ*rfc Salmonella* became ubiquitylated. In stark contrast, *Salmonella* ubiquitylation was entirely absent in cells expressing TssM^{Bp}, indicating that this protein exhibits *in trans* activity that protects cytosolic *Salmonella* (Figure 1D).

TssM is a cysteine hydrolase with specific isopeptidase activity toward polyubiquitin chains and an important *in vivo* anti-inflammatory role.[16–18] The protein is highly conserved among *B. pseudomallei* complex species, and the expression of *B. thailandensis* TssM (TssM^{Bt}) also ablated the ubiquitylation of Δ*rfc Salmonella* (Figure 1D). Consistent with an enzymatic role in hydrolyzing ubiquitin modifications, the ubiquitin-positive signal remained upon expression of the catalytically inactive variants[18] TssM^{BpC292G} or TssM^{BtC192G} (Figure 1D).

To test whether the presence of TssM explains why *B. thailandensis* does not acquire the expected ubiquitin coat, despite recruitment of RNF213, we created E555::*tssM*^{pknock} and E264::*tssM*^{pknock} mutant strains to prevent its expression. Analysis of infected cells by immunofluorescence microscopy revealed that over 70% of E264::*tssM*^{pknock} *B. thailandensis* accumulated a ubiquitin coat, compared with less than 10% of WT bacteria at 6 h post invasion (Figure 1E and S1A). E555::*tssM*^{pknock} bacteria also exhibited a significantly greater percentage of ubiquitin coating when compared to their isogenic WT strain (Figure 1E). Furthermore, immunoblotting demonstrated that E555::*tssM*^{pknock} and E264::*tssM*^{pknock} mutant bacteria, but not WT bacteria, were ubiquitylated inside infected cells and that this required RNF213 in both MEFs (Figure 1F) and HeLa cells (Figure S1B). The exogenous expression of WT, but not catalytically inactive TssM^{BtC192G}, ablated the ubiquitin-positive signal that otherwise accumulated on E264::*tssM*^{pknock} bacteria during infection (Figure 1G). We conclude that RNF213 mediates the ubiquitylation of both capsulated and non-capsulated *B. thailandensis*, but only when the bacteria lack TssM.

TssM blocks autophagy receptor recruitment

The RNF213-mediated ubiquitylation of *Salmonella* LPS,[5] GarD-deficient *Chlamydia*-containing inclusions,[4] and *Toxoplasma*-containing vacuoles[6] functions as a ubiquitin-dependent "eat-me" signal[2,19] that induces antimicrobial autophagy and pathogen elimination. However, the intracellular bacterial burden between WT and *tssM*-mutant *Burkholderia* was indistinguishable in both MEFs and RAW264.7 macrophages (Figure 2A). This finding, which is in line with previous reports for the *tssM* mutant of *B. mallei*,[18] suggests that *Burkholderia* have additional virulence mechanisms that counteract ubiquitin-mediated cell-autonomous immunity. This prompted us to test whether TssM could promote the replication of the non-cytosol adapted pathogen, *Salmonella*. Exogenous expression of WT TssM^{Bp}, but not catalytically inactive TssM^{BpC292G}, was sufficient to promote *Salmonella* replication (Figure 2B), providing further evidence that *Burkholderia* has at least one additional mechanism to block host-mediated restriction of cytosolic bacteria.

To investigate why E264::*tssM*^{pknock} bacteria, which become decorated with the ubiquitin "eat-me" signal (Figures 1E and 1F), replicate as efficiently as WT *Burkholderia*, we next analyzed the associated polyubiquitin signals. Both K63- and linear M1-linked polyubiquitin chains represent important signals for antibacterial autophagy.[20,21] At 6 h post invasion, the majority of ubiquitin-coated E264::*tssM*^{pknock} and E555::*tssM*^{pknock} bacteria (identified with an antibody that detects diverse ubiquitin chain types and mono-ubiquitin) accumulated K63- and linear M1-linked polyubiquitin chains (Figure S1C). Approximately 60% of all intracellular E264::*tssM*^{pknock} bacteria were coated with M1- or K63-linked polyubiquitin, compared to less than 5% of WT E264 bacteria, and this was dependent on RNF213 (Figures 2B and 2C). Similar findings were observed in HeLa cells (Figures S1D–S1F).

As these polyubiquitin signals initiate the recruitment of ubiquitin-binding autophagy receptors Optineurin (OPTN),[22] NDP52,[23] and p62,[24] we next explored the recruitment of these proteins to *Burkholderia*. Consistent with the accumulation of polyubiquitin signals, NDP52, p62, and OPTN were recruited to approximately 60% of E264::*tssM*^{pknock} bacteria in an RNF213-dependent manner, in contrast to fewer than 5% of WT bacteria (Figures 2E–2G). Of note, while the E555::*tssM*^{pknock} strain showed elevated marker-positive bacteria compared to WT E555, which was RNF213-dependent, it remained below 20% of total bacteria (Figures S1G–S1I). This is in line with the lower percentage of E555 bacteria that were decorated with RNF213 (Figure 1B). To test if the polysaccharide capsule of E555 bacteria limits RNF213 recruitment, we created two isogenic capsule-deficient E555 strains, E555::*wcbB*^{pknock} and E555::*wcbE*^{pknock}, and found that both demonstrated a significantly higher proportion of RNF213 coating when compared to WT E555 (Figure 2H). In the absence of TssM, the capsule-deficient strains E555::Δ*tssM*,*wcbB*^{pknock} and E555::Δ*tssM*,*wcbE*^{pknock} exhibited increased ubiquitin coating (Figure 2I) and recruitment of NDP52 (Figure 2J) when compared to the E555::Δ*tssM* strain. Our findings reveal that the capsule acts as a physical barrier for the recruitment of RNF213, and that without TssM, *B. thailandensis* has a greater propensity to become coated with polyubiquitin and associated autophagy receptors.

An additional virulence mechanism blocks autophagy initiation

The ubiquitin-dependent recruitment of autophagy receptors enables delivery of the marked "cargo" to an LC3-positive, double membrane autophagosome.[22–25] Despite our finding that individual autophagy receptors coated approximately 60% of E264::*tssM*^{pknock} bacteria, only 15% of these mutant bacteria were positive for LC3 in MEFs (Figure 2K) and less than 10% in

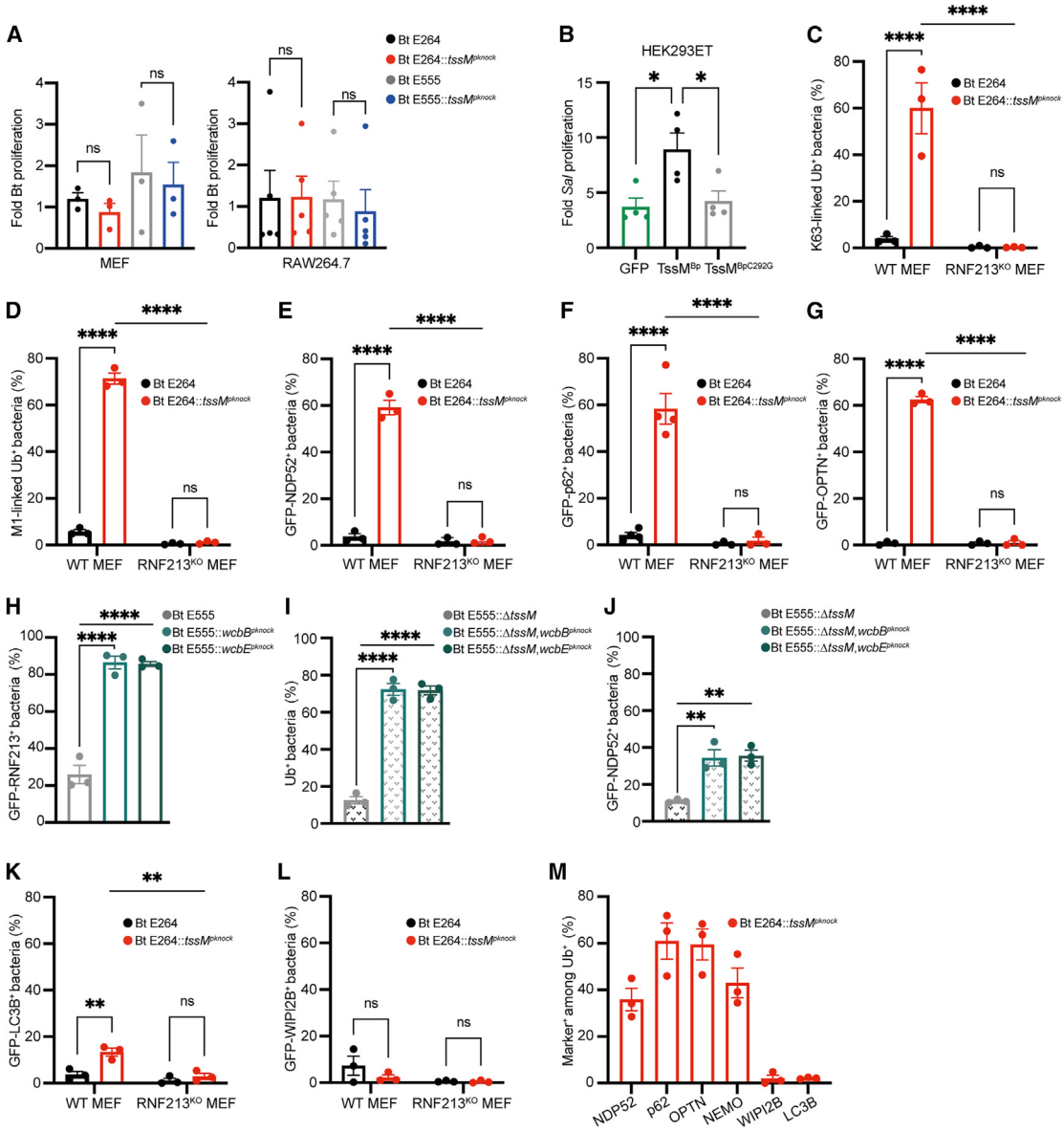

Figure 2. TssM blocks ubiquitin accumulation and autophagy receptor recruitment

(A–L) Colony forming unit assays were used to determine the fold replication at 6 h p.i. of (A) the indicated *Burkholderia* strains in MEFs or RAW264.7 macrophages, and (B) of *Salmonella* in HEK293ET cells expressing the indicated GFP-tagged protein. Quantification of the percentage of (C) K63-linked or (D) M1-linked ubiquitin-positive bacteria. Quantification of the percentage of indicated *B. thailandensis* strain colocalizing with (E) GFP-NDP52, (F) GFP-p62, (G) GFP-OPTN, (H) GFP-RNF213, (I) Ubiquitin, (J) GFP-NDP52, (K) GFP-LC3B, and (L) GFP-WIPI2B, as determined by microscopy at 6 h p.i. (M) Percentage of marker-positive *B. thailandensis* among ubiquitin-coated bacteria in WT MEFs. Data represent the mean ± SEM of at least three independent biological repeats. Statistical significance was assessed by two-way ANOVA with Tukey's multiple comparisons test (C–G, K, and L) or one-way ANOVA (A, B, H–J, and M); *$p < 0.05$; **$p < 0.01$; **** <0.0001See also Figure S1.

RAW264.7 macrophages (Figure S1J). To investigate this further, we analyzed recruitment of WIPI2B, which is required for LC3 conjugation and autophagy of *Salmonella*.[26] The percentages of WIPI2B-positive E264::*tssM*^{pknock} and WT E264 were low and indistinguishable at 6 h post invasion (Figure 2L). When marker-positive bacteria were quantified among the fraction of ubiquitin-positive E264::*tssM*^{pknock} bacteria, the failure to recruit critical autophagy proteins WIPI2B and LC3B was evident (Figure 2M). Similarly, whether quantified among the total or the ubiquitin-positive population, it was evident that WIPI2B and LC3B were associated with fewer E555::*tssM*^{pknock} bacteria than the autophagy receptors (Figure S1K–S1M). Together, this suggests that the failure in antibacterial autophagy occurs due to a block in its initiation. We propose that TssM cooperates with other effectors, including those that inhibit LC3-assisted phagocytosis and autophagy via poorly described mechanisms,[11,12] to create a multi-layered virulence mechanism that blocks the host cell-autonomous immune response.

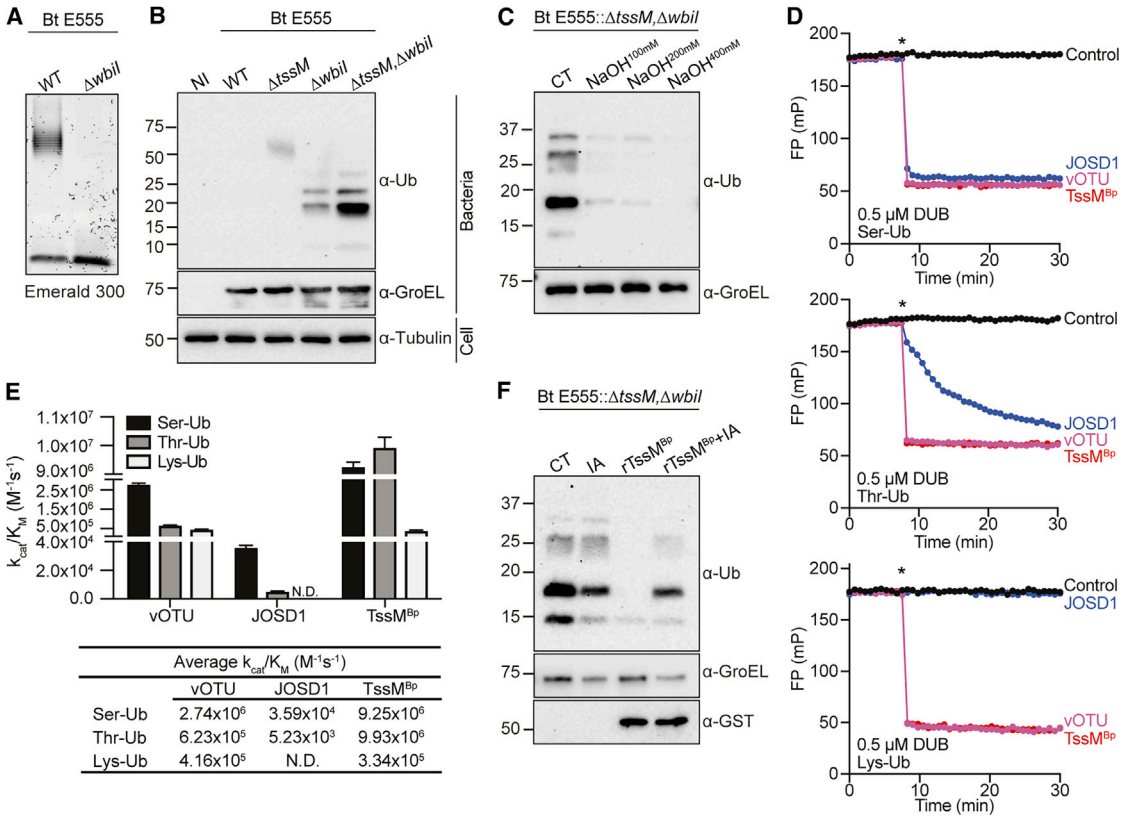

Average k_{cat}/K_M ($M^{-1}s^{-1}$)

	vOTU	JOSD1	TssM^{Bp}
Ser-Ub	$2.74x10^6$	$3.59x10^4$	$9.25x10^6$
Thr-Ub	$6.23x10^5$	$5.23x10^3$	$9.93x10^6$
Lys-Ub	$4.16x10^5$	N.D.	$3.34x10^5$

Figure 3. TssM is a ubiquitin esterase that hydrolyzes ubiquitylated LPS

(A) Emerald 300 stain of LPS from indicated *B. thailandensis* strains grown in Luria broth (LB).

(B) Immunoblot analysis of *B. thailandensis* strains isolated from infected MEFs, 24 h p.i.

(C) Bacteria isolated from MEFs infected with the E555::Δ*wbil,*Δ*tssM* strain were lysed and incubated with 100, 200, or 400 mM NaOH for 30 min prior to immunoblot analysis. CT: non-treated control.

(D) Representative FP data monitoring cleavage of Rho-S(Ub)G (Ser-Ub), Rho-T(Ub)G (Thr-Ub), and Tamra-K(Ub)G (Lys-Ub) substrates following addition of the DUB (indicated by an asterisk).

(E) Catalytic efficiencies (mean ± SEM of three repeats) for all enzyme-substrate combinations, with the exception of JOSD1, which had no detectable isopeptidase activity.

(F) Bacteria isolated from MEFs infected with the E555::Δ*wbil,*Δ*tssM* strain were incubated with recombinant His-GST-tagged TssM$^{Bp\Delta N191}$ (rTssM^{Bp}) +/− iodoacetamide (IA) for 30 min prior to immunoblot analysis. Data representative of three biological repeats (A–D and F).

See also Figure S2

LPS represents the ubiquitylated substrate

As RNF213 ubiquitylates *Salmonella* LPS, rather than a proteinaceous substrate,[5] we therefore hypothesized that the RNF213-dependent ubiquitylation of *tssM*^{pknock} bacteria also represented modification of bacterial LPS. To test this, we created an E555::Δ*wbil* mutant or an E555::Δ*tssM*,Δ*wbil* double mutant, in which the lack of WbiI prevents formation of long O-antigen, leaving only the lipid A and inner core of the LPS moiety (Figure 3A). Surprisingly, a defined, lower molecular weight ubiquitin-positive banding pattern was detected in LPS-enriched lysates from the E555::Δ*wbil*-infected cells (Figure 3B). This suggested that deleting the O-antigen removes a physical barrier to the ubiquitylation of *B. thailandensis,* perhaps by providing better access to the lipid A moiety. This ubiquitin-positive banding pattern resembled that detected for the Δ*rfc* mutant of *Salmonella* (Figure 1C) and importantly, ubiquitylation of the E555::Δ*tssM*,Δ*wbil* double mutant was enhanced compared to the E555::Δ*wbil* mutant (Figure 3B).

The strict correlation between the molecular weight of the detected ubiquitin signal and O-antigen size strongly suggests the direct and non-canonical ester-linked ubiquitylation of *B. thailandensis* LPS on available hydroxyl groups,[27] as seen for *Salmonella*.[5] Indeed, treatment of E555::Δ*tssM*,Δ*wbil* bacteria isolated from infected cells with increasing concentrations of sodium hydroxide, which selectively hydrolyzes ester-linked conjugates over amide-linked ubiquitylation,[5] clearly resulted in progressive loss of the ubiquitin signature (Figure 3C). Therefore, we conclude that without TssM, *Burkholderia* undergo RNF213-mediated non-canonical ubiquitylation of LPS.

TssM is a highly potent ubiquitin esterase

TssM has reported isopeptidase activity,[18] cleaving amide bonds within a polyubiquitin chain, yet our data imply that TssM reverses ester-linked ubiquitylation. To test whether TssM exhibits both isopeptidase and esterase activity, as seen for several other members of the ubiquitin-specific protease

(USP) family of DUBs,[28] we purified recombinant His-GST-tagged TssM$^{Bp\Delta N191}$. This variant lacks the first 191 amino acids but contains the intact catalytic domain.[18] When incubated with the activity-based probe, Ub-Propargylamide (Ub-PA),[29] a shift in molecular mass, indicative of a covalent interaction between the probe and TssM, demonstrated that TssM$^{Bp\Delta N191}$ represented an active enzyme (Figure S2A). As models for the analysis of esterase activity, we synthesized substrates containing ubiquitin linked to the hydroxyl group of Serine (Ser) or Threonine (Thr), as well as the isopeptide-linked Tamra-K(Ub)G (Lys-Ub)[30] as a control substrate. Cleavage of these substrates was monitored by a decrease in fluorescence polarization (FP) following release of the fluorescent Ser/Thr/Lys-containing peptide from ubiquitin. As expected, the human ester-specific DUB JOSD1[28] preferred the Rho-S(Ub)G and Rho-T(Ub)G substrates (hereafter referred to as Ser-Ub and Thr-Ub) over isopeptide-linked Lys-Ub, whereas the Crimean-Congo Hemorrhagic Fever Virus DUB, vOTU,[31] cleaved all ubiquitin modifications indiscriminately (Figures 3D, S2B, and S2C). TssM cleaved both ester- and isopeptide-linked ubiquitin substrates very efficiently, even at low or subnanomolar enzyme concentrations (Figures 3D and S2D). In fact, TssM exhibited extremely robust ubiquitin esterase activity, with catalytic efficiencies approaching 1 × 10^7 $M^{-1}s^{-1}$ against the Ser- and Thr-linked ubiquitin substrates (Figure 3E). Compared to the Lys-Ub substrate, TssM was nearly 30-fold more active toward ester-linked ubiquitin, whereas the control enzyme vOTU showed just a 4-fold preference. Remarkably, TssM demonstrated up to 1900-fold more activity toward ester-linked Ub than JOSD1, making it a highly potent ubiquitin esterase. This provides direct evidence that TssM exhibits both isopeptidase and esterase activity.

Given the esterase activity of TssM, we tested whether recombinant TssM$^{Bp\Delta N191}$ directly removed ubiquitin from bacterial LPS. Treatment of E555::Δ*tssM*,Δ*wbil* lysates obtained from infected cells with TssM$^{Bp\Delta N191}$ removed the ubiquitin signal otherwise detected in control conditions, or when iodoacetamide (an established inhibitor of cysteine-dependent DUBs) was included in the reaction (Figure 3F). Similar results were obtained when Δ*rfc Salmonella* lysates from infected cells were treated with TssM$^{Bp\Delta N191}$ (Figure S2E). We conclude that TssM enzymatically hydrolyzed ester-linked ubiquitylated LPS from both *Burkholderia* and *Salmonella*, providing a physiological function for its esterase activity.

Molecular basis for TssM activity

We determined a 2.5 Å crystal structure of TssM$^{Bp\Delta N191}$ covalently bound to Ub at its active site to visualize the molecular basis for ubiquitin esterase activity (Figures 4A, S3A–S3C, and Table S1). The structure of TssM revealed a bacterial Ig-like domain 5 (Big5) fold N-terminal to a catalytic USP-type DUB module (Figure 4A). Ig-like domains facilitate protein or ligand interactions,[32] and we detected unexplained electron density in the β1 groove, indicating the possibility of a co-purified ligand from expression in *E. coli* (Figures S3D and S3E). A recently reported crystal structure of TssM corroborates this overall architecture and includes additional N-terminal residues that form a β1 strand and, in one example, mediate a dimeric strand swap within the crystal.[33] When TssM was overexpressed in cells, however, the Big5 domain was not required for deubiquitylation of LPS (Figure S3F). USP domains are typically composed of six conserved "box" regions that can be interrupted by sequence insertions of varying lengths.[34] The TssM USP domain is very minimal and contains no sequence insertions. Boxes 1, 2, 5, and 6 are well conserved and form the core USP module, including the catalytic triad (Figures 4B and S3G–S3I). Ubiquitin is typically bound at the S1 substrate-binding site by a set of "fingers" encoded within Boxes 3 and 4, as well as a Box 4 "blocking loop" that guides the ubiquitin C-terminus into the active site. In contrast, TssM has no recognizable finger structure and compensates for an extremely short Box 4 region by encoding an analogous blocking loop within Box 6 instead (Figures 4B and S3G–S3I).

Within the TssM active site lies an aligned Cys-His-Asp catalytic triad, as well as a conserved Asn that forms the oxyanion hole (Figure 4C). Mutation of these sites ablated or diminished isopeptidase activity toward a Lys-Ub substrate, but interestingly, the acidic Asp or oxyanion hole Asn were not required for ubiquitin esterase activity (Figures 4D, 4E, S4A, and S4B). Among USPs, the length of the so-called Cys-loop that precedes that catalytic Cys is almost perfectly conserved. TssM encodes a one amino acid insertion within the Cys-loop (Figure 4F), but its truncation had a minimal effect on esterase activity and instead, ΔL287 specifically reduced isopeptidase function (Figures 4G, 4H, S4A, and S4C). As the ubiquitin C-terminus threads into the active site, TssM coordinates the basic R42, R72, and R74 residues of ubiquitin with acidic residues E362 and E469 in Boxes 2 and 6, respectively (Figure 4I). Mutation of either residue severely diminished isopeptidase activity, but esterase activity was more significantly impacted by an inability to coordinate R42 and R72 with residue E469 (Figures 4J, 4K, S4A, and S4D). Lastly, the remainder of the S1 site is composed of hydrophobic interactions to the I44 hydrophobic patch of ubiquitin stemming from TssM Boxes 3 and 6 (Figure 4L). Mutations in these hydrophobic TssM residues (Y402, F459, or V466) reduced esterase activity to varying extents and ablated isopeptidase function (Figures 4M, 4N, S4A, and S4E).

As we noted that several of our structure-guided mutations in the TssM active site or S1 site affected isopeptidase function more so than esterase, we sought to determine if any had completely lost isopeptidase activity. We selected N286A, E362R, F459A, V466R, and E469R as TssM mutants that more significantly impacted isopeptidase activity (Figures 4C–4N and S4A–S4E). At higher enzyme concentrations, all mutants tested were able to cleave the Lys-Ub substrate efficiently except V466R and E469R, which were severely impaired (Figure S4F). We selected TssM V466R for further characterization, as it retained more esterase activity compared with E469R. Despite a ~100-fold reduction in the k_{cat}/K_M for Ser-Ub and Thr-Ub substrates, the V466R mutant exhibited a ~21,000-fold reduction in k_{cat}/K_M for Lys-Ub, amounting to a ~5,000-fold specificity for ester- over isopeptide-linked substrates (Figures 5A and S4G). Based on this identified specificity, a TssM V466R mutant cleaved an ester-linked ubiquitylated maltoheptaose substrate generated by the E3 ligase HOIL-1,[35] but not an isopeptide-linked di-ubiquitin chain (Figure 5B). We suggest that TssM esterase activity is more compatible with weak or transient substrate encounters, with the differential dependency on certain active site features allowing us to uncouple esterase

CellPress
OPEN ACCESS

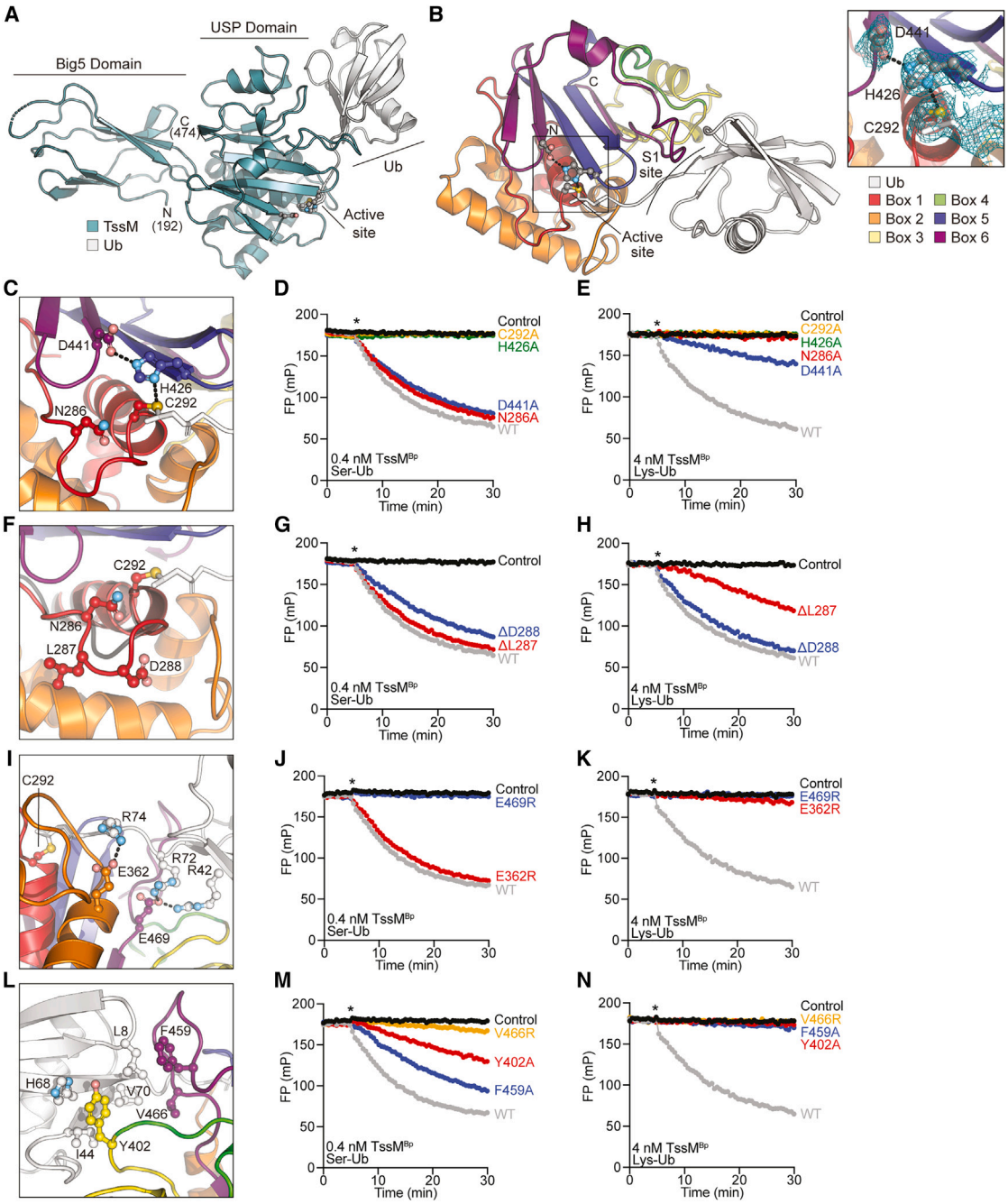

Figure 4. Structural basis of TssM^{Bp} esterase activity

(A) Crystal structure of TssM$^{Bp\Delta N191}$ (teal) bound to Ub (gray).

(B) Close-up of the TssM USP domain colored by box regions 1–6, with Ub (gray) shown in the S1 site. Representative 2|Fo|-|Fc| electron density is shown at 1s.

(C–E) TssM catalytic triad C292, H426, and D441, as well as the oxyanion hole N286 are shown. Hydrogen bonds are shown as dashed lines. Effects of mutation on TssM activity are shown for (D) Ser-Ub and (E) Lys-Ub substrates.

(F–H) The extended TssM Cys-loop (red) in comparison to a typical USP Cys-loop (gray). Activity data for TssM truncations ΔL287 and ΔD288 are shown for (G) Ser-Ub and (H) Lys-Ub substrates.

(I–K) Coordination of the Ub C-terminus and R42 by TssM E362 and E469. Activity data of E362R and E469R mutants are shown for (J) Ser-Ub and (K) Lys-Ub substrates.

(L–N) Coordination of the Ub I44 hydrophobic patch by TssM S1 site residues Y402, F459, and V466 is shown. The effects of mutations on cleavage of (M) Ser-Ub and (N) Lys-Ub are shown.

In all panels, DUB addition is indicated by an asterisk. WT and control data in (D) and (G), (E) and (H), (J) and (M), and (K) and (N) are identical and reproduced for clarity as data were collected in the same experiment. All FP data shown represent mean ± SEM of three biological repeats.

See also Figure S3 and S4 and Table S1

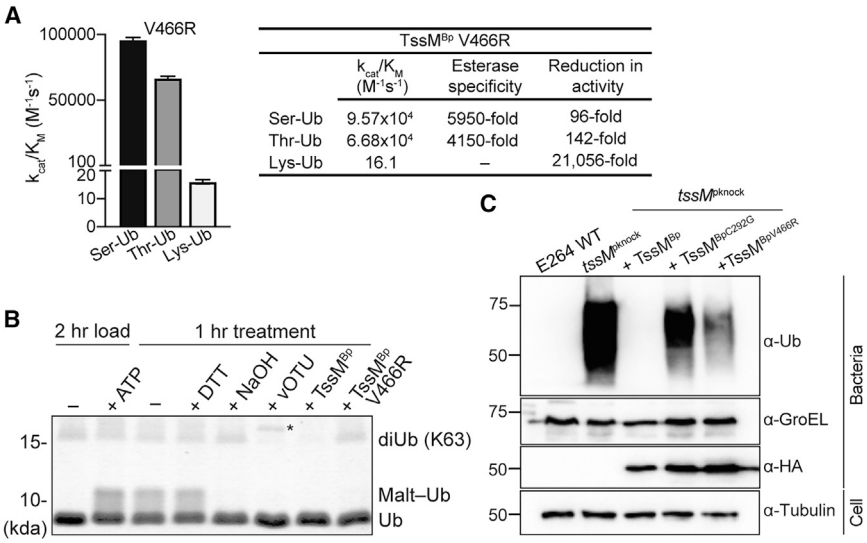

Figure 5. Esterase-specific activity of the TssM^{Bp} V466R mutant

(A) Rate constants and correlating catalytic efficiency (k_{cat}/K_M) derived for esterase-specific TssM^{BpΔN191} V466R are shown as mean ± SEM of three biological repeats.

(B) Chemical and enzymatic treatment of K63-linked di-ubiquitin and ester-linked ubiquitylated maltoheptaose. HOIL-1 was used to assemble ubiquitylated maltoheptaose, and samples of the reaction were treated with reducing agent, base, the nonspecific vOTU (marked with an asterisk), or the indicated TssM variants.

(C) Immunoblot analysis of indicated *B. thailandensis* strains isolated from infected WT MEFs at 24 h p.i. Data representative of three biological repeats (B and C).

See also Figure S4

and isopeptidase activity. To test the importance of esterase activity in infection conditions, we analyzed the extent of LPS ubiquitylation upon infection with *tssM* mutant bacteria expressing HA-tagged WT TssM, a catalytic mutant or the esterase-specific variant of TssM (V466R). As expected, *tssM* mutant bacteria accumulated a ubiquitin smear, which was abolished upon expression of WT TssM and partially reduced upon expression of TssM-V466R (Figure 5C). Thus, the ubiquitin esterase activity of TssM reverses RNF213-dependent ubiquitylation of *Burkholderia* LPS.

Conservation of ubiquitin esterase activity

Next, we asked how common esterase activity is among an array of bacterial DUBs. As observed with human DUBs,[28] many bacterial DUBs were capable of ubiquitin esterase activity at high (0.5 μM) enzyme concentration (Figure 6A). Despite their expected activities toward the Ub-PA probe (Figure S4H), among a panel of N-terminal GFP-tagged full-length bacterial DUBs, only TssM protected *Salmonella* from LPS ubiquitylation *in trans* (Figure 6B). Furthermore, recombinant TssM was the most potent DUB tested, removing all anti-ubiquitin detected bands from E555::Δ*tssM*,Δ*wbil* bacteria isolated from infected cells (Figure 6C). This revealed a specificity within TssM, compared with several other bacterial DUBs, for the removal of ubiquitin from LPS.

To extend our analysis of substrate specificity, we specifically examined a subset of bacterial peptidases from the C19 family, of which TssM is a member. Using MEROPS, we selected C19 peptidases from intracellular bacteria including other *Burkholderia* species, *Parachlamydia acanthamoebae*,[39] *Simkania negevensis*,[40] and *Waddlia chondrophila*[41] (protein sequences aligned[42] in Figure S5) and tested whether they could cleave ubiquitylated LPS when expressed *in trans*. Of these, only peptidases from *Burkholderia* blocked the ubiquitylation of *Salmonella* LPS (Figure 6D). We then used NCBI BLAST against the *B. pseudomallei* TssM and identified an additional putative orthologue conserved in several species of *Chromobacterium* (Figure S6A), a Gram-negative bacterium associated with rare opportunistic infections that involve growth in the host cell cytosol.[43–45] Surprisingly, despite only 33% sequence conservation with TssM^{Bp}, expression of the *Chromobacterium* orthologue, denoted as TssM^{Cs}, protected *Salmonella* from host-mediated ubiquitylation, indicative of esterase activity (Figure 6D). Recombinant TssM^{Cs} protein was active on all fluorescent substrates tested (Figures 6E and S6B) and exhibited over 100-fold greater activity toward the ester-linked substrates than the isopeptide substrate (Figures 6F and 6G). Finally, as recombinant TssM^{Cs} hydrolyzed ubiquitin from the LPS of E555::Δ*tssM*,Δ*wbil* (Figure 6H), we compared the AlphaFold model[46,47] of TssM^{Cs} to our TssM structure to assess structural homology (Figures 6I, S6C, and S6D). Consistent with similar activities toward ubiquitylated LPS, there was considerable alignment between the active site regions where the AlphaFold model confidence was highest. Together, these findings suggest that ubiquitin esterase activity is encoded by at least two cytosolic bacteria as a mechanism of countering RNF213 defenses.

DISCUSSION

Our finding that some conserved bacterial DUBs are esterases that selectively reverse the ubiquitylation of a non-canonical substrate reveals a previously undescribed molecular mechanism for the evasion of RNF213-mediated cell-autonomous immunity. As the ubiquitin-coating of bacteria is pro-inflammatory,[20] and given that TssM deubiquitylates at least two K63-linked proteinaceous substrates, TRAF6 and TRAF3,[17] TssM represents the only known bacterial DUB to exhibit dual isopeptidase and esterase activity targeting both protein and lipid substrates to dampen the host's pro-inflammatory immune response. Without the activity of TssM, *B. pseudomallei* infection of mice induced elevated pro-inflammatory cytokine production and more rapid death of the animal,[17] demonstrating the importance of TssM's activity.

Interestingly, TssM is conserved in the human disease-causing *B. mallei* and *B. pseudomallei*, as well as *B. thailandensis*, which rarely causes disease in humans. We therefore hypothesize that

CellPress
OPEN ACCESS

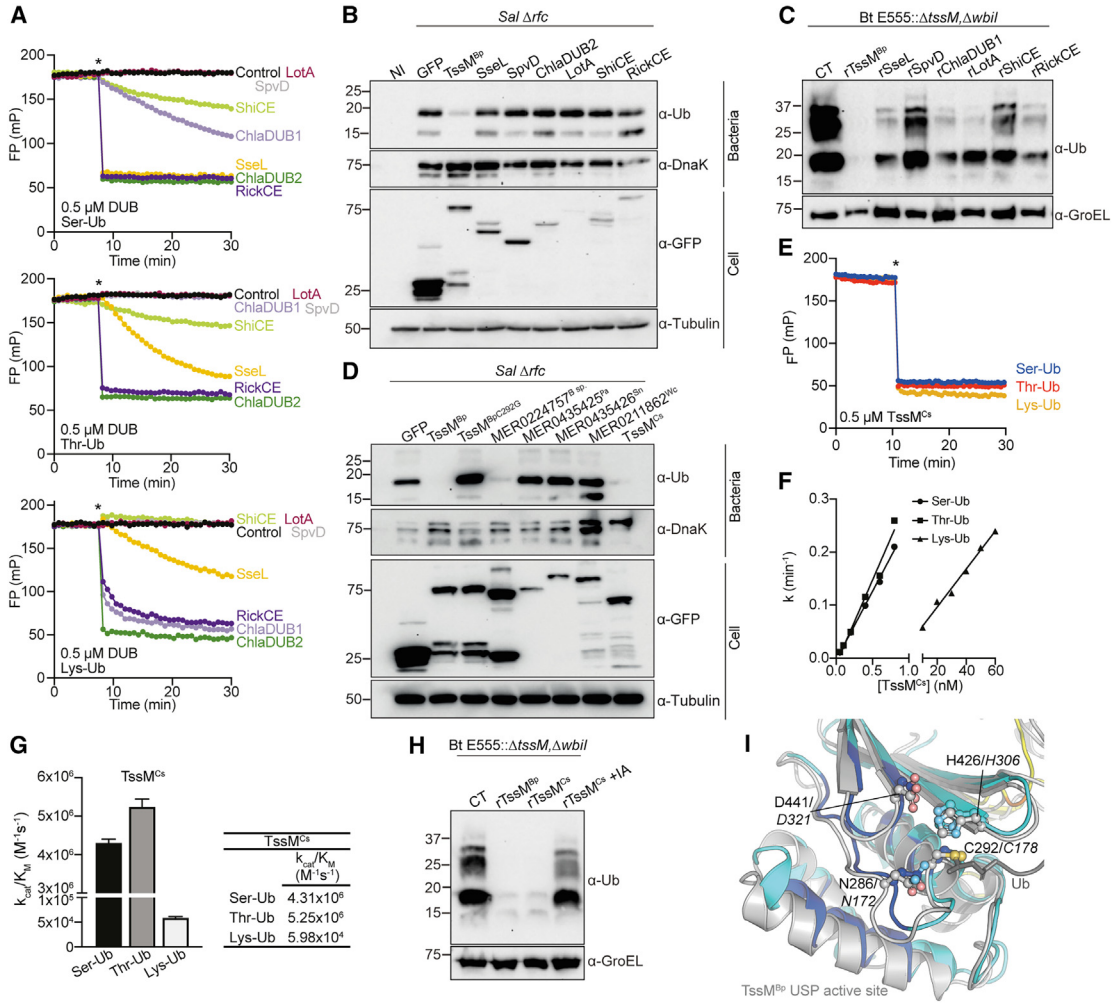

Figure 6. Esterase activity in other bacterial peptidases

(A) Representative FP data monitoring cleavage of Ser-Ub, Thr-Ub, and Lys-Ub substrates following addition of the DUB (indicated by an asterisk).

(B) Immunoblot analysis of Δ*rfc Salmonella* isolated at 6 h p.i. from infected HEK293ET cells transiently expressing the indicated GFP-tagged bacterial cysteine hydrolases. The panel includes SseL and SpvD from *Salmonella*,[36,37] ChlaDUB1 and ChlaDUB2 from *Chlamydia*,[37] LotA from *Legionella*,[38] ShiCE from *Shigella,* and RickCE from *Rickettsia*.[37]

(C) Bt E555::Δ*tssM,*Δ*wbil* mutant bacteria isolated from infected MEF cells were treated with 0.5 μM of the indicated purified bacterial DUB.

(D) Immunoblot analysis of Δ*rfc Salmonella* isolated from infected cells expressing the indicated GFP-tagged putative C19 peptidases of *Burkholderia* (*B sp.*), *Parachlamydia acanthamoebae* (*Pa*), *Simkania negevensis* (*Sn*), *Waddlia chondrophila* (*Wc*), and *Chromobacterium sinusclupearum* (*Cs*).

(E–G) Representative FP data monitoring cleavage of Ser-Ub, Thr-Ub, and Lys-Ub substrates with 0.5 μM TssM^{Cs}. Data were collected in triplicate and (F) rate constants and (G) catalytic efficiency of the TssM^{Cs} protein toward each substrate are shown as mean ± SEM.

(H) Immunoblot analysis of E555::Δ*tssM,*Δ*wbil B. thailandensis* isolated from infected MEFs and incubated with control (CT), recombinant His-GST-tagged TssM^{BpΔN191} (rTssM^{Bp}) or TssM^{Cs} +/− iodoacetamide (IA) for 30 min.

(I) Structural alignment of the active site of TssM (gray) and the AlphaFold model of TssM^{Cs} (colored) showing similarity between the two proteins surrounding the active site. Catalytic residues for TssM are labeled, with aligned residues in TssM^{Cs} labeled in italics. rTssM^{Bp} refers to recombinant His-GST-tagged TssM^{BpΔN191} (C and H). Data representative of three biological repeats (A–F and H) or mean ± SEM of three biological repeats (G).

See also Figures S5 and S6

TssM in *B. thailandensis* remains under selective pressure through its encounter with non-human hosts. Both *B. pseudomallei* and *B. thailandensis* are found in soil and are phagocytosed by free-living amebae,[48] but there is no known homolog of RNF213 in amebae. Perhaps more noteworthy then is that TssM is highly conserved among the cytosol-dwelling *Burkholderia pseudomallei* complex species, suggesting it is under selective pressure when the bacterium enters this host environment compared to *Burkholderia cepacia* complex species that reside in the vacuole and rarely encode for TssM.

For cytosolic *Burkholderia* spp., we propose that at least three mechanisms cooperate to counteract RNF213. First, the capsule provides a physical barrier consistent with acapsular *B. pseudomallei* exhibiting a significant reduction in virulence.[49] Second, TssM directly reverses RNF213-mediated LPS ubiquitylation. Lastly, the initiation of autophagy is blocked

in a TssM-independent manner. The multiple layers of protection suggest that overcoming this mechanism of host immunity is of utmost importance for replication in the host cell cytosol.

While many DUBs have esterase activity *in vitro,*[28] our work describes the biological importance of TssM's ubiquitin esterase activity. Our findings raise the possibility that other enzymes with esterase activity mediate the regulation of non-canonical and/or non-proteinaceous ubiquitylated substrates in disease and beyond. To this end, our highly specific TssM esterase variant provides a valuable tool for future studies that investigate non-canonical ubiquitylation.

STAR★METHODS

Detailed methods are provided in the online version of this paper and include the following:

- KEY RESOURCES TABLE
- RESOURCE AVAILABILITY
  - Lead contact
  - Materials availability
  - Data and code availability
- EXPERIMENTAL MODELS AND PARTICIPANT DETAILS
  - Cell culture
  - Bacterial strains
- METHOD DETAILS
  - Bacterial infections
  - Bacterial isolation prior to immunoblotting
  - Bacterial mutagenesis
  - DNA plasmids and cloning
  - Immunofluorescence microscopy
  - *In vitro* DUB assay
  - Fluorescence polarization DUB assays
  - Protein expression and purification
  - SDS-PAGE and immunoblotting
  - Synthesis of ester-linked substrates
  - TssM crystallization and structure analysis
  - Ubiquitylated maltoheptaose assay
- QUANTIFICATION AND STATISTICAL ANALYSIS

SUPPLEMENTAL INFORMATION

Supplemental information can be found online at https://doi.org/10.1016/j.chom.2024.04.012.

ACKNOWLEDGMENTS

We thank Prof. David Holden and Dr Jo Stevens for scientific discussion, members of the Thurston and Pruneda laboratories for protocols and feedback, and Jose Penades, Peter Hill, and Alex McCarthy for scientific discussion, comments and reading of the manuscript. We are grateful to Dr. Felix Randow, who provided RNF213^{KO} MEFs, RNF213^{KO} HeLa cells, and cells expressing GFP:RNF213 as well as plasmids for the expression of GFP-tagged OPTN, p62, NDP52, and LC3B; the Defense Science and Technology Laboratory (DSTL) of Porton Down, who provided *B. thailandensis* E264, E555, and associated strains; and Prof. Richard Titball, who provided E264 bacteria. pKnock, pdm4, and associated protocols were provided by Dr. Sariqa Wagley. pDAI-SceI-SacB was a gift from Miguel Valvano (Addgene plasmid # 113635), and Dr. Sara Buhrlage provided the JOSD1 expression vector. Anti-*Burkholderia* antibody was provided by the United States Army Medical Research Institute of Infectious Diseases, an agency of the US Government ("USAMRIID"). We thank the Diamond Light Source (Oxford, United Kingdom) for synchrotron access and Marc Morgan from the Center of Structural Biology at Imperial College for data collection.The funders had no role in study design, data collection and analysis, decision to publish, or preparation of the manuscript. A National Institute of General Medical Sciences funding grant R35GM142486 (J.N.P.), a Biotechnology and Biological Sciences Research Council David Phillips Fellowship BB/R011834/1 (T.L.M.T., F.B.) and a Wellcome Trust Investigator Award to David Holden, 209411/Z/17/Z (M.S.) funded this work.

AUTHOR CONTRIBUTIONS

M.S. performed and analyzed experiments leading to the discovery that TssM removes ubiquitin from LPS. M.S. expressed, purified, and obtained TssM crystals, and J.N.P. resolved the structure. M.S. analyzed the C19 peptidases and other bacterial DUBs for activity toward LPS-Ub and identified the activity of TssM^{Cs} with contributions from F.B. M.S., Y.H., F.B., and F.K. performed and analyzed the association of ubiquitin and autophagy markers to bacteria, and M.S. and F.B. performed CFU assays. V.P. and P.P.G. generated the ubiquitin FP substrates, and R.E.L. carried out the FP assays and purification and analysis of TssM mutants as well as recombinant DUBs. B.W. created constructs and analyzed TssM *in vitro* DUB activity. T.L.M.T. and M.S. designed the original study, and J.N.P. made important conceptual contributions. M.S., R.E.L., J.N.P., and T.L.M.T. wrote the manuscript.

DECLARATION OF INTERESTS

The authors declare no competing interests.

Received: February 14, 2024
Revised: March 15, 2024
Accepted: April 11, 2024
Published: June 12, 2024

REFERENCES

1. Huang, S., Meng, Q., Maminska, A., and MacMicking, J.D. (2019). Cell-autonomous immunity by IFN-induced GBPs in animals and plants. Curr. Opin. Immunol. *60*, 71–80. https://doi.org/10.1016/J.COI.2019.04.017.
2. Randow, F., MacMicking, J.D., and James, L.C. (2013). Cellular Self-Defense: How Cell-Autonomous Immunity Protects Against Pathogens. Science *340*, 701–706. https://doi.org/10.1126/SCIENCE.1233028.
3. Thery, F., Martina, L., Asselman, C., Zhang, Y., Vessely, M., Repo, H., Sedeyn, K., Moschonas, G.D., Bredow, C., Teo, Q.W., et al. (2021). Ring finger protein 213 assembles into a sensor for ISGylated proteins with antimicrobial activity. Nat. Commun. *12*, 5772. https://doi.org/10.1038/S41467-021-26061-W.
4. Walsh, S.C., Reitano, J.R., Dickinson, M.S., Kutsch, M., Hernandez, D., Barnes, A.B., Schott, B.H., Wang, L., Ko, D.C., Kim, S.Y., et al. (2022). The bacterial effector GarD shields Chlamydia trachomatis inclusions from RNF213-mediated ubiquitylation and destruction. Cell Host Microbe *30*, 1671–1684.e9. https://doi.org/10.1016/j.chom.2022.08.008.
5. Otten, E.G., Werner, E., Crespillo-Casado, A., Boyle, K.B., Dharamdasani, V., Pathe, C., Santhanam, B., and Randow, F. (2021). Ubiquitylation of lipopolysaccharide by RNF213 during bacterial infection. Nature *594*, 111–116. https://doi.org/10.1038/s41586-021-03566-4.
6. Hernandez, D., Walsh, S., Saavedra Sanchez, L., Dickinson, M.S., and Coers, J. (2022). Interferon-Inducible E3 Ligase RNF213 Facilitates Host-Protective Linear and K63-Linked Ubiquitylation of Toxoplasma gondii Parasitophorous Vacuoles. mBio *13*, e0188822. https://doi.org/10.1128/MBIO.01888-22.
7. Ahel, J., Lehner, A., Vogel, A., Schleiffer, A., Meinhart, A., Haselbach, D., and Clausen, T. (2020). Moyamoya disease factor RNF213 is a giant E3 ligase with a dynein-like core and a distinct ubiquitin-transfer mechanism. Elife *9*, 561855–e56223. https://doi.org/10.7554/elife.56185.
8. Limmathurotsakul, D., Golding, N., Dance, D.A.B., Messina, J.P., Pigott, D.M., Moyes, C.L., Rolim, D.B., Bertherat, E., Day, N.P.J., Peacock, S.J., and Hay, S.I. (2016). Predicted global distribution of Burkholderia pseudomallei and burden of melioidosis. Nat. Microbiol. *1*, 15008–15015. https://doi.org/10.1038/nmicrobiol.2015.8.

9. Harley, V.S., Dance, D.A., Drasar, B.S., and Tovey, G. (1998). Effects of Burkholderia pseudomallei and other Burkholderia species on eukaryotic cells in tissue culture. Microbios *96*, 71–93.

10. Meumann, E.M., Limmathurotsakul, D., Dunachie, S.J., Wiersinga, W.J., and Currie, B.J. (2024). Burkholderia pseudomallei and melioidosis. Nat. Rev. Microbiol. *22*, 155–169. https://doi.org/10.1038/S41579-023-00972-5.

11. Gong, L., Cullinane, M., Treerat, P., Ramm, G., Prescott, M., Adler, B., Boyce, J.D., and Devenish, R.J. (2011). The Burkholderia pseudomallei Type III Secretion System and BopA Are Required for Evasion of LC3-Associated Phagocytosis. PLoS One *6*, e17852. https://doi.org/10.1371/journal.pone.0017852.

12. Heacock-Kang, Y., McMillan, I.A., Norris, M.H., Sun, Z., Zarzycki-Siek, J., Bluhm, A.P., Cabanas, D., Norton, R.E., Ketheesan, N., Miller, J.F., et al. (2021). The Burkholderia pseudomallei intracellular 'TRANSITome. Nat. Commun. *12*, 1907–1912. https://doi.org/10.1038/s41467-021-22169-1.

13. Kovacs-Simon, A., Hemsley, C.M., Scott, A.E., Prior, J.L., and Titball, R.W. (2019). Burkholderia thailandensis strain E555 is a surrogate for the investigation of Burkholderia pseudomallei replication and survival in macrophages. BMC Microbiol. *19*, 97. https://doi.org/10.1186/S12866-019-1469-8.

14. Bayliss, M., Donaldson, M.I., Nepogodiev, S.A., Pergolizzi, G., Scott, A.E., Harmer, N.J., Field, R.A., and Prior, J.L. (2017). Structural characterisation of the capsular polysaccharide expressed by Burkholderia thailandensis strain E555:: wbil (pKnock-KmR) and assessment of the significance of the 2-O-acetyl group in immune protection. Carbohydr. Res. *452*, 17–24. https://doi.org/10.1016/J.CARRES.2017.09.011.

15. Vander Broek, C.W., and Stevens, J.M. (2017). Type III Secretion in the Melioidosis Pathogen Burkholderia pseudomallei. Front. Cell. Infect. Microbiol. *7*, 255. https://doi.org/10.3389/FCIMB.2017.00255.

16. Burtnick, M.N., Brett, P.J., and DeShazer, D. (2014). Proteomic Analysis of the Burkholderia pseudomallei Type II Secretome Reveals Hydrolytic Enzymes, Novel Proteins, and the Deubiquitinase TssM. Infect. Immun. *82*, 3214–3226. https://doi.org/10.1128/IAI.01739-14.

17. Tan, K.S., Chen, Y., Lim, Y.-C., Tan, G.-Y.G., Liu, Y., Lim, Y.-T., MacAry, P., and Gan, Y.-H. (2010). Suppression of Host Innate Immune Response by Burkholderia pseudomallei through the Virulence Factor TssM. J. Immunol. *184*, 5160–5171. https://doi.org/10.4049/JIMMUNOL.0902663.

18. Shanks, J., Burtnick, M.N., Brett, P.J., Waag, D.M., Spurgers, K.B., Ribot, W.J., Schell, M.A., Panchal, R.G., Gherardini, F.C., Wilkinson, K.D., and Deshazer, D. (2009). Burkholderia mallei tssM encodes a putative deubiquitinase that is secreted and expressed inside infected RAW 264.7 murine macrophages. Infect. Immun. *77*, 1636–1648. https://doi.org/10.1128/iai.01339-08.

19. Perrin, A.J., Jiang, X., Birmingham, C.L., So, N.S.Y., and Brumell, J.H. (2004). Recognition of bacteria in the cytosol of mammalian cells by the ubiquitin system. Curr. Biol. *14*, 806–811. https://doi.org/10.1016/j.cub.2004.04.033.

20. Noad, J., Von Der Malsburg, A., Pathe, C., Michel, M.A., Komander, D., and Randow, F. (2017). LUBAC-synthesized linear ubiquitin chains restrict cytosol-invading bacteria by activating autophagy and NF-κB. Nat. Microbiol. *2*, 17063. https://doi.org/10.1038/NMICROBIOL.2017.63.

21. Thurston, T.L., Boyle, K.B., Allen, M., Ravenhill, B.J., Karpiyevich, M., Bloor, S., Kaul, A., Noad, J., Foeglein, A., Matthews, S.A., et al. (2016). Recruitment of TBK1 to cytosol-invading Salmonella induces WIPI2-dependent antibacterial autophagy. EMBO J. *35*, 1779–1792. https://doi.org/10.15252/EMBJ.201694491.

22. Wild, P., Farhan, H., McEwan, D.G., Wagner, S., Rogov, V.V., Brady, N.R., Richter, B., Korac, J., Waidmann, O., Choudhary, C., et al. (2011). Phosphorylation of the autophagy receptor optineurin restricts Salmonella growth. Science *333*, 228–233. 1979. https://doi.org/10.1126/science.1205405.

23. Thurston, T.L.M., Ryzhakov, G., Bloor, S., von Muhlinen, N., and Randow, F. (2009). The tbk1 adaptor and autophagy receptor ndp52 restricts the proliferation of ubiquitin-coated bacteria. Nat. Immunol. *10*, 1215–1221. https://doi.org/10.1038/ni.1800.

24. Zheng, Y.T., Shahnazari, S., Brech, A., Lamark, T., Johansen, T., and Brumell, J.H. (2009). The adaptor protein p62/SQSTM1 targets invading bacteria to the autophagy pathway. J. Immunol. *183*, 5909–5916. https://doi.org/10.4049/jimmunol.0900441.

25. Nakagawa, I., Amano, A., Mizushima, N., Yamamoto, A., Yamaguchi, H., Kamimoto, T., Nara, A., Funao, J., Nakata, M., Tsuda, K., et al. (2004). Autophagy defends cells against invading group A Streptococcus. Science *306*, 1037–1040. 1979. https://doi.org/10.1126/science.1103966.

26. Thurston, T.L., Boyle, K.B., Allen, M., Ravenhill, B.J., Karpiyevich, M., Bloor, S., Kaul, A., Noad, J., Foeglein, A., Matthews, S.A., et al. (2016). Recruitment of TBK1 to cytosol-invading Salmonella induces WIPI2-dependent antibacterial autophagy. EMBO J. *35*, 1779–1792. https://doi.org/10.15252/embj.201694491.

27. Sengyee, S., Yoon, S.H., West, T.E., Ernst, R.K., and Chantratita, N. (2019). Lipopolysaccharides from Different Burkholderia Species with Different Lipid A Structures Induce Toll-Like Receptor 4 Activation and React with Melioidosis Patient Sera. Infect. Immun. *87*, e00692-19. https://doi.org/10.1128/IAI.00692-19.

28. de Cesare, V., Carbajo Lopez, D., Mabbitt, P.D., Fletcher, A.J., Soetens, M., Antico, O., Wood, N.T., and Virdee, S. (2021). Deubiquitinating enzyme amino acid profiling reveals a class of ubiquitin esterases. Proc. Natl. Acad. Sci. USA *118*, e2006947118. https://doi.org/10.1073/pnas.2006947118.

29. Ekkebus, R., Van Kasteren, S.I., Kulathu, Y., Scholten, A., Berlin, I., Geurink, P.P., De Jong, A., Goerdayal, S., Neefjes, J., Heck, A.J.R., et al. (2013). On terminal alkynes that can react with active-site cysteine nucleophiles in proteases. J. Am. Chem. Soc. *135*, 2867–2870. https://doi.org/10.1021/ja309802n.

30. Geurink, P.P., El Oualid, F., Jonker, A., Hameed, D.S., and Ovaa, H. (2012). A General Chemical Ligation Approach Towards Isopeptide-Linked Ubiquitin and Ubiquitin-Like Assay Reagents. Chembiochem *13*, 293–297. https://doi.org/10.1002/CBIC.201100706.

31. Akutsu, M., Ye, Y., Virdee, S., Chin, J.W., and Komander, D. (2011). Molecular basis for ubiquitin and ISG15 cross-reactivity in viral ovarian tumor domains. Proc. Natl. Acad. Sci. USA *108*, 2228–2233. https://doi.org/10.1073/pnas.1015287108.

32. Bodelón, G., Palomino, C., and Fernández, L.Á. (2013). Immunoglobulin domains in Escherichia coli and other enterobacteria: from pathogenesis to applications in antibody technologies. FEMS Microbiol. Rev. *37*, 204–250. https://doi.org/10.1111/J.1574-6976.2012.00347.X.

33. Hermanns, T., Uthoff, M., Baumann, U., and Hofmann, K. (2024). The structural basis for deubiquitination by the fingerless USP-type effector TssM. Life Sci. Alliance *7*, e202302422. https://doi.org/10.26508/Lsa.202302422.

34. Eletr, Z.M., and Wilkinson, K.D. (2014). Regulation of proteolysis by human deubiquitinating enzymes. Biochim. Biophys. Acta *1843*, 114–128. https://doi.org/10.1016/J.BBAMCR.2013.06.027.

35. Kelsall, I.R., McCrory, E.H., Xu, Y., Scudamore, C.L., Nanda, S.K., Mancebo-Gamella, P., Wood, N.T., Knebel, A., Matthews, S.J., and Cohen, P. (2022). HOIL-1 ubiquitin ligase activity targets unbranched glucosaccharides and is required to prevent polyglucosan accumulation. EMBO J. *41*, e109700. https://doi.org/10.15252/embj.2021109700.

36. Grabe, G.J., Zhang, Y., Przydacz, M., Rolhion, N., Yang, Y., Pruneda, J.N., Komander, D., Holden, D.W., and Hare, S.A. (2016). The Salmonella effector SpvD is a cysteine hydrolase with a serovar-specific polymorphism influencing catalytic activity, suppression of immune responses, and bacterial virulence. J. Biol. Chem. *291*, 25853–25863. https://doi.org/10.1074/jbc.M116.752782.

37. Pruneda, J.N., Durkin, C.H., Geurink, P.P., Ovaa, H., Santhanam, B., Holden, D.W., and Komander, D. (2016). The Molecular Basis for Ubiquitin and Ubiquitin-like Specificities in Bacterial Effector Proteases. Mol. Cell *63*, 261–276. https://doi.org/10.1016/J.MOLCEL.2016.06.015.

38. Warren, G.D., Kitao, T., Franklin, T.G., Nguyen, J.V., Geurink, P.P., Kubori, T., Nagai, H., and Pruneda, J.N. (2023). Mechanism of Lys6 poly-ubiquitin specificity by the L. pneumophila deubiquitinase LotA. Mol. Cell *83*, 105–120.e5. https://doi.org/10.1016/j.molcel.2022.11.022.

39. Greub, G. (2009). Parachlamydia acanthamoebae, an emerging agent of pneumonia. Clin. Microbiol. Infect. *15*, 18–28. https://doi.org/10.1111/J.1469-0691.2008.02633.X.

40. Vouga, M., Baud, D., and Greub, G. (2017). Simkania negevensis, an insight into the biology and clinical importance of a novel member of the Chlamydiales order. Crit. Rev. Microbiol. *43*, 62–80. https://doi.org/10.3109/1040841X.2016.1165650.

41. Baud, D., Thomas, V., Arafa, A., Regan, L., and Greub, G. (2007). Waddlia chondrophila, a Potential Agent of Human Fetal Death. Emerg. Infect. Dis. *13*, 1239–1243. https://doi.org/10.3201/EID1308.070315.

42. Waterhouse, A.M., Procter, J.B., Martin, D.M.A., Clamp, M., and Barton, G.J. (2009). Jalview Version 2—a multiple sequence alignment editor and analysis workbench. Bioinformatics *25*, 1189–1191. https://doi.org/10.1093/BIOINFORMATICS/BTP033.

43. O'hara-Hanley, K., Harrison, A., and Soby, S.D. (2022). Chromobacterium alticapitis sp. nov. and Chromobacterium sinusclupearum sp. nov. isolated from wild cranberry bogs in the Cape Cod National Seashore, USA. Int. J. Syst. Evol. Microbiol. *72*. https://doi.org/10.1099/IJSEM.0.005410.

44. Batista, J.H., and Neto, J.F. da S. (2017). Chromobacterium violaceum pathogenicity: Updates and insights from genome sequencing of novel Chromobacterium species. Front Microbiol *8*. https://doi.org/10.3389/fmicb.2017.02213.

45. Du, J., Reeves, A.Z., Klein, J.A., Twedt, D.J., Knodler, L.A., and Lesser, C.F. (2016). The type III secretion system apparatus determines the intracellular niche of bacterial pathogens. Proc Natl Acad Sci U S A *113*, 4794–4799. https://doi.org/10.1073/pnas.1520699113.

46. Varadi, M., Anyango, S., Deshpande, M., Nair, S., Natassia, C., Yordanova, G., Yuan, D., Stroe, O., Wood, G., Laydon, A., et al. (2022). AlphaFold Protein Structure Database: massively expanding the structural coverage of protein-sequence space with high-accuracy models. Nucleic Acids Res. *50*, D439–D444. https://doi.org/10.1093/NAR/GKAB1061.

47. Jumper, J., Evans, R., Pritzel, A., Green, T., Figurnov, M., Ronneberger, O., Tunyasuvunakool, K., Bates, R., Žídek, A., Potapenko, A., et al. (2021). Highly accurate protein structure prediction with AlphaFold. Nature *96*, 583–589. https://doi.org/10.1038/s41586-021-03819-2.

48. Inglis, T.J., Rigby, P., Robertson, T.A., Dutton, N.S., Henderson, M., and Chang, B.J. (2000). Interaction between Burkholderia pseudomallei and Acanthamoeba Species Results in Coiling Phagocytosis, Endamebic Bacterial Survival, and Escape. Infect. Immun. *68*, 1681–1686. https://doi.org/10.1128/IAI.68.3.1681-1686.2000.

49. Atkins, T., Prior, R., Mack, K., Russell, P., Nelson, M., Prior, J., Ellis, J., Oyston, P.C.F., Dougan, G., and Titball, R.W. (2002). Characterisation of an acapsular mutant of Burkholderia pseudomallei identified by signature tagged mutagenesis. J. Med. Microbiol. *51*, 539–553. https://doi.org/10.1099/0022-1317-51-7-539.

50. Aubert, D.F., Hamad, M.A., and Valvano, M.A. (2014). A markerless deletion method for genetic manipulation of Burkholderia cenocepacia and other multidrug-resistant gram-negative bacteria. Methods Mol. Biol. *1197*, 311–327. https://doi.org/10.1007/978-1-4939-1261-2_18.

51. Randow, F., and Sale, J.E. (2006). Retroviral transduction of DT40. Subcell. Biochem. *40*, 383–386. https://doi.org/10.1007/978-1-4020-4896-8_30.

52. Pruneda, J.N., Bastidas, R.J., Bertsoulaki, E., Swatek, K.N., Santhanam, B., Clague, M.J., Valdivia, R.H., Urbé, S., and Komander, D. (2018). A Chlamydia effector combining deubiquitination and acetylation activities induces Golgi fragmentation. Nat. Microbiol. 2018 *3*, 1377–1384. https://doi.org/10.1038/s41564-018-0271-y.

53. Geurink, P.P., Van Tol, B.D.M., Van Dalen, D., Brundel, P.J.G., Mevissen, T.E.T., Pruneda, J.N., Elliott, P.R., Van Tilburg, G.B.A., Komander, D., and Ovaa, H. (2016). Development of Diubiquitin-Based FRET Probes To Quantify Ubiquitin Linkage Specificity of Deubiquitinating Enzymes. Chembiochem *17*, 816–820. https://doi.org/10.1002/CBIC.201600017.

54. van Tol, B.D.M., van Doodewaerd, B.R., Lageveen-Kammeijer, G.S.M., Jansen, B.C., Talavera Ormeño, C.M.P., Hekking, P.J.M., Sapmaz, A., Kim, R.Q., Moutsiopoulou, A., Komander, D., et al. (2023). Neutron-encoded diubiquitins to profile linkage selectivity of deubiquitinating enzymes. Nat. Commun. 2023 *14*, 1661–1714. https://doi.org/10.1038/s41467-023-37363-6.

55. Wilkinson, K.D., Gan-Erdene, T., and Kolli, N. (2005). Derivitization of the C-terminus of ubiquitin and ubiquitin-like proteins using intein chemistry: Methods and uses. Methods Enzymol. *399*, 37–51. https://doi.org/10.1016/s0076-6879(05)99003-4.

56. Winter, G., Waterman, D.G., Parkhurst, J.M., Brewster, A.S., Gildea, R.J., Gerstel, M., Fuentes-Montero, L., Vollmar, M., Michels-Clark, T., Young, I.D., et al. (2018). DIALS: Implementation and Evaluation of a New Integration Package*74*, pp. 85–97. urn:issn:2059-7983. https://doi.org/10.1107/S2059798317017235.

57. Evans, P.R., and Murshudov, G.N. (2013). How Good Are My Data and what Is the Resolution?*69*, pp. 1204–1214. Urn:issn:0907-4449. https://doi.org/10.1107/S0907444913000061.

58. Potterton, L., Agirre, J., Ballard, C., Cowtan, K., Dodson, E., Evans, P.R., Jenkins, H.T., Keegan, R., Krissinel, E., Stevenson, K., et al. (2018). CCP4i2: the new graphical user interface to the CCP4 program suite. Acta Crystallogr. D Struct. Biol. *74*, 68–84. https://doi.org/10.1107/S2059798317016035.

59. McCoy, A.J., Grosse-Kunstleve, R.W., Adams, P.D., Winn, M.D., Storoni, L.C., and Read, R.J. (2007). Phaser crystallographic software. J. Appl. Crystallogr. *40*, 658–674. https://doi.org/10.1107/S0021889807021206.

60. Vijay-kumar, S., Bugg, C.E., and Cook, W.J. (1987). Structure of ubiquitin refined at 1.8 A resolution. J. Mol. Biol. *194*, 531–544. https://doi.org/10.1016/0022-2836(87)90679-6.

61. Cowtan, K. (2006). The Buccaneer software for automated model building. 1. Tracing protein chains. Acta Crystallogr. D Biol. Crystallogr. *62*, 1002–1011. https://doi.org/10.1107/S0907444906022116.

62. Adams, P.D., Afonine, P.V., Bunkóczi, G., Chen, V.B., Davis, I.W., Echols, N., Headd, J.J., Hung, L.W., Kapral, G.J., Grosse-Kunstleve, R.W., et al. (2010). PHENIX: a comprehensive Python-based system for macromolecular structure solution. Acta Crystallogr. D Biol. Crystallogr. *66*, 213–221. https://doi.org/10.1107/S0907444909052925.

63. Emsley, P., Lohkamp, B., Scott, W.G., and Cowtan, K. (2010). Features and development of Coot. urn:issn:0907-4449 *66*, 486–501. https://doi.org/10.1107/S0907444910007493.

STAR★METHODS

KEY RESOURCES TABLE

REAGENT or RESOURCE	SOURCE	IDENTIFIER
Antibodies		
Mouse monoclonal anti Tubulin beta	DSHB	Cat#E7; RRID: AB_528499
Mouse monoclonal anti DnaK (clone 8E2/2)	Enzo Life Science	Cat#ADI-SPA-880; RRID: AB_2039064
Rat monoclonal anti GFP	Proteintech	Cat#3H9-100; RRID: AB_10773374
Goat polyclonal anti GroEL	Antibodies-Online	Cat#ABIN6292975
Mouse monoclonal anti Ubiquitin (clone FK2)	Enzo Life Science	Cat#BML-PW8810; RRID: AB_10541840
Mouse monoclonal anti Ubiquitin (clone UBCJ2)	Enzo Life Science	Cat#ENZ-ABS840; RRID: AB_2935893
Rabbit polyclonal anti GST	Sigma	Cat#G7781; RRID: AB_259965
Goat anti-Rabbit (HRP-conjugated)	Agilent (Dako)	Cat#P0448; RRID: AB_2617138
Goat anti-Mouse (HRP-conjugated)	Agilent (Dako)	Cat#P0447; RRID: AB_2617137
Donkey anti-Goat (HRP-conjugated)	Abcam	Cat#ab6885; RRID: AB_955423
Goat anti-Rat (HRP-conjugated)	Cell Signaling Technology	Cat#7077; RRID: AB_10694715
Rabbit monoclonal anti M1-Ubiquitin (clone 1E3)	Merck	Cat#ZRB2114; RRID: AB_2938573
Rabbit monoclonal anti K63-Ubiquitin (clone Apu3)	Millipore	Cat#05-1308; RRID: AB_1587580
Mouse monoclonal anti LC3	Cosmo Bio	Cat#CTB-LC3-2-IC; RRID: AB_10707197
Rabbit polyclonal anti-Burkholderia (GB18)	Gift from USAMRIID	N/A
Donkey anti mouse IgG (Alexa Fluor 555)	Thermo Fisher Scientific	Cat#A-31570; RRID: AB_2536180
Donkey anti mouse IgG (Alexa Fluor 488)	Thermo Fisher Scientific	Cat#A-21202; RRID: AB_141607
Donkey anti rabbit IgG (Alexa Fluor 488)	Thermo Fisher Scientific	Cat#A-21206; RRID: AB_2535792
Bacterial and Virus Strains		
Salmonella enterica serovar Typhimurium, wild-type strain	NCTC	NCTC: 12023
Δ*rfc* mutant of *Salmonella* (12023)	Gift from Felix Randow	N/A
Bt E264: *Burkholderia thailandensis,* strain E264; Acapsular	Gift from Dstl	N/A
Bt E555: *Burkholderia thailandensis*, strain E555; Capsulated	Gift from Dstl	N/A
Bt E264 + pRFP: E264 WT strain carrying the pHR4-GroS-RFP plasmid	Gift from Dstl	N/A
Bt E555 + pRFP: E555 WT strain carrying the pHR4-GroS-RFP plasmid	Gift from Dstl	N/A
Bt E264:*tssM*^{pknock}: pKnock-E264-*tssM* plasmid integrated in the BTH_II0854 locus	This paper	N/A
Bt E264:*tssM*^{pknock} + pRFP: Strain carrying the pHR4-GroS-RFP plasmid	This paper	N/A

(*Continued on next page*)

Continued

REAGENT or RESOURCE	SOURCE	IDENTIFIER
Bt E555:*tssM*^{pknock}: pKnock-E555-*tssM* plasmid integrated in the RS0119175 locus	This paper	N/A
Bt E555:*tssM*^{pknock} + pRFP: Strain carrying the pHR4-GroS-RFP plasmid	This paper	N/A
Bt E555:Δ*tssM*: Strain harboring a deletion of *tssM* gene (RS0119175)	This paper	N/A
Bt E555:Δ*wbiI*: Strain harboring a deletion of *wbiI* gene (RS0101800)	This paper	N/A
Bt E555:Δ*tssM*,Δ*wbiI*: Strain harboring a deletion of *tssM* (RS0119175) and *wbiI* (RS0101800)	This paper	N/A
Bt E555:*wcbB*^{pknock}: E555 with pKnock-*wcbB* plasmid integrated in *wcbB* locus	This paper	N/A
Bt E555:*wcbE*^{pknock}: E555 with pKnock-*wcbE* plasmid integrated in *wcbE* locus	This paper	N/A
Bt E555:Δ*tssM*,*wcbB*^{pknock}: E555 *tssM* mutant with pKnock plasmid integrated in *wcbB* locus	This paper	N/A
Bt E555:Δ*tssM*,*wcbE*^{pknock}: E555 *tssM* mutant with pKnock plasmid integrated in *wcbE* locus	This paper	N/A
Bt E264:*tssM*^{pknock} + pHR4-GroS-TssM^{Bp} *tssM* mutant strain carrying vector for expression of HA-tagged WT TssM^{Bp}, TssM^{BpC292G} or TssM^{BpV466R}	This paper	N/A
Chemicals, Peptides, and Recombinant Proteins		
Lipofectamine 2000	Life Technologies	Cat#116680
GFP-TRAP	Pierce	Cat#gta-100
Protease inhibitors	Roche	Cat#04693132001
PhosStop	Roche	Cat#04906837001
Iodoacetamide	Sigma	Cat# I1149
Aqua-Poly/Mount	Polysciences	Cat#18606
Bug Buster Protein Extraction Reagent	Merck	Cat#70584
Doxycycline Hyclate	Merck	Cat#D5207
Quick Coomassie stain	Molecular Dimensions	Cat#GEN-QC-STAIN
HisPur™ Ni-NTA resin	ThermoFisher	Cat#88222
Glutathione agarose	Pierce	Cat#16100
Ub-Propargylamide (Ub-PA)	Ref. 29	N/A
Rho-S(Ub)G (Ser-Ub)	This paper	N/A
Rho-T(Ub)G (Thr-Ub)	This paper	N/A
Tamra-K(Ub)G (Lys-Ub)	Ref. 30	N/A
Critical Commercial Assays		
Pro-Q™ Emerald 300 Lipopolysaccharide Gel Stain Kit	Thermo Fisher	Cat#P20495
Deposited data		
Crystal Structure of TssM^{Bp}-Ub	This paper	PDB: 8SSI
Experimental Models: Cell Lines		
HEK293ET	Gift from Felix Randow	RRID: CVCL_6996
MEF	Gift from Felix Randow	RRID: CVCL_L690
MEF RNF213 ^{KO}	Gift from Felix Randow	N/A
MEF RNF213 ^{KO} expressing GFP-RNF213	Gift from Felix Randow	N/A
MEF WT and RNF213 ^{KO} stably expressing GFP-NDP52	This paper	N/A
MEF WT and RNF213 ^{KO} stably expressing GFP-p62	This paper	N/A
MEF WT and RNF213 ^{KO} stably expressing GFP-OPTN	This paper	N/A
MEF WT and RNF213 ^{KO} stably expressing GFP-LC3B	This paper	N/A

(*Continued on next page*)

Continued

REAGENT or RESOURCE	SOURCE	IDENTIFIER
MEF WT and RNF213 ^{KO} stably expressing GFP-WIPI2B	This paper	N/A
HeLa	Gift from Felix Randow	RRID: CVCL_0030
HeLa RNF213 ^{KO}	Gift from Felix Randow	N/A
RAW264.7	ATCC	Cat#TIB-71; RRID: CVCL_0493
Experimental Models: Organisms/Strains		
E. coli DH5α	Thermo Fisher	Cat#18265017
E. coli TOP10	Thermo Fisher	N/A
E. coli Rosetta (DE3)	Millipore	Cat#70954
E. coli BL21 (DE3)	New England	Cat#C2527
E. coli CC118 λpir	Lab collection strain provided by K. Timmis	N/A
E. coli S17-1 λpir	Lab collection strain provided by K. Timmis	N/A
Oligonucleotides		
See Table S2 for a complete list of oligonucleotides	This paper	N/A
Recombinant DNA		
M6p-derived plasmids for retroviral transduction: GFP-NDP52, GFP-p62, GFP-OPTN, GFP-LC3B and GFP-WIPI2B	Gift from Felix Randow	N/A
pKnock-KmR	Gift from S. Wagley	N/A
pKnock-E264-*tssM*: 700-800 bp internal fragment of Bt E264 BTH_II0854 gene cloned into pKnock via NotI/SalI sites	This paper	N/A
pKnock-E555-*tssM*: 700-800 bp internal fragment of Bt E555 RS0119175 gene cloned into pKnock via NotI/SalI sites	This paper	N/A
pKnock-*wcbB*: 700-800 bp internal fragment of Bt E555 RS0102180 gene cloned into pKnock via NotI/SalI sites	This paper	N/A
pKnock-*wcbE*: 700-800 bp internal fragment of Bt E555 RS0102150 gene cloned into pKnock via NotI/XhoI sites	This paper	N/A
pDM4	Gift from S. Wagley	N/A
pDM4-E555-*tssM*-I-SceI: 500 bp up- and downstream of Bt E555 RS0119175 gene cloned into pDM4 via XbaI/SpeI sites. Plasmid harboring an I-SceI endonuclease site	This paper	N/A
pDM4-E555-*wbiI*-I-SceI: 500 bp up- and downstream of Bt E555 RS0101800 gene cloned into pDM4 via XbaI/SpeI sites. Plasmid harboring an I-SceI endonuclease site	This paper	N/A
pDAI-SceI-sacB	Gift from Miguel Valvano, ref. 50	Addgene plasmid Cat#113635
pBHR4-GroS-TssM^{Bp}: bacterial expression with Cter HA-tag	This paper	N/A
pBHR4-GroS-TssM$^{Bp\text{-}C292G}$: bacterial expression with Cter HA-tag	This paper	N/A
pBHR4-GroS-TssM$^{Bp\text{-}V466R}$: bacterial expression with Cter HA-tag	This paper	N/A

(*Continued on next page*)

Continued

REAGENT or RESOURCE	SOURCE	IDENTIFIER
Plasmids for protein expression, see Table S2	This paper	N/A
Plasmids for mammalian expression, see Table S2	This paper	N/A
Software and Algorithms		
Prism	GraphPad Version 9	https://www.graphpad.com/scientific-software/prism/
Image Lab	BioRad	https://www.bio-rad.com/en-uk/product/image-lab-software?ID=KRE6P5E8Z
Adobe Illustrator	Adobe creative cloud	https://www.adobe.com/uk/creativecloud.html
Jalview	Ref. 39	Version 2.11.3.2
MARS	BMG Labtech	Version 3.32
Dials	Ref. 56	Version 3.10
CCP4i2	Ref. 58	Version 7.1.004
Phaser	Ref. 59	Version 2.8.3
Buccaneer	Ref. 61	Version 1.5
PHENIX	Ref. 62	Version 1.17.1
Coot	Ref. 63	Version 0.9
PyMol	Version 2.2.2	www.pymol.org

RESOURCE AVAILABILITY

Lead contact

Further information and requests for resources and reagents should be directed to and will be fulfilled by the lead contact, Teresa L.M. Thurston (t.thurston@imperial.ac.uk).

Materials availability

Plasmids and cell lines generated in this study are available upon request to the lead contact.

Data and code availability

Coordinates and structure factors for the TssM-Ub structure have been deposited in the Protein DataBank under accession code 8SSI and will be publicly available from the date of publication. All other data are available in the main text of supplementary materials. This paper does not report original code. Any additional information required to reanalyse the data reported in this paper is available from the lead contact upon request.

EXPERIMENTAL MODELS AND PARTICIPANT DETAILS

Cell culture

HEK293ET (originating from a female fetus), MEFs, RNF213^{KO} MEFs, RNF213^{KO} MEFs expressing GFP-RNF213, HeLa, RNF213^{KO} HeLa (all provided by Dr Felix Randow) and RAW264.7 macrophages (ATCC, originating from a tumor in a male mouse) were maintained in Dulbecco's modified Eagle's medium (DMEM; Sigma) supplemented with 10% fetal calf serum (FCS; GIBCO, Life Technologies) at 37°C in 5% CO_2. In 24 well-plates, cells were transfected using Lipofectamine 2000 (Life Technologies, Inc.) as per the manufacturer's instructions. HEK293ET seeded in 10 cm dishes, were transfected using calcium phosphate two days prior infection. Stable cell lines were generated by retroviral transduction with M6P-derived plasmids encoding GFP-NDP52, GFP-p62, GFP-OPTN, GFP-LC3B and GFP-WIPI2B. 48 h post transduction, cells were either selected in blasticidin (5 μg/mL) or sorted by flow cytometry (GFP$^+$ cells).

Bacterial strains

Escherichia coli strain DH5α was used for cloning (Thermo Fisher), and BL21 (DE3) (New England) and Rosetta (DE3) (Millipore) for protein expression. *E. coli CC118* λpir and E. coli S17-1 λpir were used for construction of λpir-dependent vectors and conjugal transfer respectively. *Salmonella enterica* serovar Typhimurium strain NCTC 12023 was used with Δ*rfc* provided by Dr Felix Randow. *B. thailandensis* acapsular E264 and capsulated E555, as well as associated fluorescent RFP strains (carrying pHR4-GroS-RFP), were provided by the Defense Science and Technology Laboratory of Porton Down. Bacterial growth conditions are described in the appropriate methods sections below.

METHOD DETAILS

Bacterial infections

S. Typhimurium strains were grown overnight in LB and subcultured (1:33) in fresh LB for 3.5 h prior to infection at 37°C. For analysis of extracted intracellular bacteria, HEK293ET or MEF cells were seeded in a 10 cm dish and infected with 1 mL of bacterial subculture for 15 min at 37°C. After two or three PBS washes, cells were incubated in 100 μg/mL gentamicin for 1 h, after which the medium was changed to 20 μg/mL gentamicin for the rest of the infection. To enumerate intracellular *Salmonella* by colony forming unit assay, cells in a 12-well plate were infected with 14 μL of undiluted subculture for 15 min at 37°C. After two PBS washes, the cells were incubated in DMEM supplemented with 10% FCS and 100 μg/mL gentamicin for 2 h, prior to incubation in 20 μg/mL gentamicin. At the desired time point post invasion, cells from triplicate wells were lysed in 1 mL cold PBS with 0.1% Triton X-100 and serial dilutions plated in duplicate on LB agar.

Burkholderia strains were grown overnight in LB and subcultured (1:20) in fresh LB for 3.5 h (optical density of 1.8–2 at 600 nm) prior to infection at 37°C. For analysis of extracted intracellular bacteria, cells seeded in a 10 cm dish were infected with 100 μL of bacterial subculture. Following centrifugation at 800 × *g* for 5 min, cells were incubated for 2 h at 37°C to allow bacterial invasion. The cells were then washed two or three times with warm PBS and maintained in fresh media containing 100 μg/mL imipenem for the remaining time of infection. For the enumeration of colony forming units, MEFs were infected with subcultured bacteria at an MOI of 100 for 2 h and RAW264.7 macrophages infected at an MOI of 10 with an overnight culture for 1 h at 37°C following centrifugation at 800 × *g* for 5 min. After three PBS washes, cells were maintained in DMEM supplemented with 10% FCS and 100 μg/mL imipenem for the duration of the experiment. Cells from triplicate wells were lysed with 1 mL cold PBS containing 0.1% Triton X-100 and plated in duplicate onto LB agar.

Bacterial isolation prior to immunoblotting

To analyze ubiquitylation of bacteria as previously described,[5] infected cells, at 4 h post-invasion for *Salmonella* and 24 h post-invasion for *Burkholderia,* were lysed in 5 mL of cold lysis buffer (1% Triton X-100, 30 mM HEPES (pH 7.5), 100 mM NaCl, 10 mM $MgCl_2$, 10 mM Iodoacetamide and complete protease inhibitor cocktail (Roche)) for 5 min. After a sample was collected for analysis by immunoblot with anti-tubulin (or anti-GFP antibodies when required), lysates were centrifuged at 300 × *g* for 5 min. The bacteria-containing supernatant was collected and centrifuged at 16,100 × *g* for 10 min at 4°C. The bacterial pellets were washed with lysis buffer and lysed in 50 μL of BugBuster (Merck) supplemented with 10 mM Iodoacetamide and protease inhibitor cocktail. After 5 min of lysis at room temperature, bacterial lysates were centrifuged at 16,100 × *g*, and the supernatant was either directly mixed with Laemmli buffer (for DnaK and GroEL immunoblots) or heat-cleared (90°C for 15 min) and centrifuged at 16,100 × *g* for 10 min to further purify ubiquitylated LPS prior to analysis by immunoblot with an anti-ubiquitin antibody.

Bacterial mutagenesis

To generate mutants in *B. thailandensis*, two different approaches were used. For gene disruption by targeted insertion of a pknock plasmid into the chromosome, an internal fragment of TssM (700-800bp) was amplified by PCR from B*. thailandensis* DNA using primers with engineered NotI and SalI restriction sites. The TssM-pKnock plasmid was introduced into *B*. *thailandensis* E264 or E555 strains via conjugation from *E*. *coli* S17-1 λ*pir.* Conjugants were selected on LB agar with kanamycin/gentamicin and pknock integration in the correct locus was verified by colony PCR.

In-frame deletions of TssM and WbiI were created using the pDM4 suicide vector. A 1 kb fragment containing 500 bp upstream and downstream of the gene of interest was generated by overlap PCR and ligated into pDM4 via its XbaI and SpeI sites. The pDM4 vectors were further modified to insert an I-SceI recognition site that allows generation of a site-specific DNA double-strand break by the I-SceI endonuclease[50] and sequence verified using pDM4-F and pDM4-R primers. The generated pDM4 plasmids were introduced into *B*. *thailandensis* via conjugation from *E*. *coli* S17-1 λ*pir* and colonies selected on LB agar with chloramphenicol and gentamicin. To increase the probability of a second recombination event, the pDAI-SceI-SacB plasmid[50] was transferred by conjugation into the single crossover mutants. Double crossover (chloramphenicol-sensitive colonies) mutants were obtained upon selection with tetracycline and gentamicin. The genotype of the mutants was confirmed by PCR, after which bacteria were grown on salt-free LB agar containing 10% (w/v) sucrose for pDAI-SceI-SacB plasmid counter-selection.

DNA plasmids and cloning

ptCMV plasmids were used for transient expression in mammalian cells. M6P plasmids were used to produce recombinant murine leukemia virus for stable expression in mammalian cells.[51] Either pETM30 or pOPINB was used for protein expression in *E. coli*. C19 peptidases, with MEROPS identifiers MER0224757, MER0435425, MER0435426 and MER0211862 were gene synthesised (Invitrogen GeneArt Strings DNA Fragments). The *Burkholderia pseudomallei* genes for Uniprot proteins, Q63K38 (BapA), Q63K40 (BapC), Q63K50 (BopC), Q63K41 (BopE), Q63K45 (BprD), Q63KH5 (CHBP), Q63MX4 (VgrG5) and Q63K53 (TssM) were amplified from K96243 gDNA, provided by Dr Jo Stevens. Mutations and gene truncations were generated by polymerase chain reaction and products were confirmed by DNA sequencing. Table S2 details the primers and plasmids used and generated in this study.

Immunofluorescence microscopy

Cells were seeded on coverslips one day prior to infection at a density of $5x10^4$ or $1x10^5$ cells/well. For GFP-RNF213 MEFs, protein expression was induced with 1 μg/mL doxycycline for at least 15 h prior to infection. Cells were infected using an MOI of 100 as described above for *Burkholderia.* At the indicated time point, cells were washed twice in PBS, fixed using 3% paraformaldehyde (PFA) for 15 min at room temperature and incubated in a quenching solution (50 mM NH_4Cl) for 10 min. Cells were then permeabilized in 0.1% Triton X-100-PBS and incubated with appropriate primary and secondary antibodies (with DAPI) for 1 h. Samples were then mounted onto glass slides using Aqua-Poly/Mount (Polysciences, Inc.) and visualised using a confocal laser scanning microscope (LSM 710, Carl Zeiss) equipped with a Plan Apochromat 63× (Carl Zeiss) oil-immersion objective. Images were analyzed with ImageJ. For scoring, at least 100 individual bacteria were blind scored from duplicate coverslips by at least two independent scorers.

In vitro DUB assay

Following the infection of cells as described above, bacterial pellets, containing ubiquitylated-LPS, were washed and resuspended in 50 mM Tris (pH 7.4), 50 mM NaCl, 5 mM DTT and treated with the indicated purified DUB, diluted in 25 mM Tris (pH 7.4), 150 mM NaCl, 10 mM DTT at 0.5 μM +/− 10 mM Iodoacetamide for 30 min at 37°C. Bacterial pellets were then lysed in Bugbuster and analyzed by immunoblot as described above.

Fluorescence polarization DUB assays

FP was monitored using a BMG Labtech CLARIOstar microplate reader. Reaction volumes were 20 μL and data were collected in a black, low-protein binding 384-well plate at 22°C, blanked against fresh FP buffer containing 25 mM HEPES (pH 7.4), 150 mM NaCl, 0.1 mg/mL BSA, 5 mM β-mercaptoethanol. For the ester-linked substrates conjugated to a rhodamine110 fluorophore, 482-16 nm and 530-40 nm optic filters were used for excitation and emission, respectively. For the isopeptide-linked Tamra-K(Ub)G substrate, the Tamra fluorophore was excited at 540-20 nm and emission was monitored at 590-20 nm. In each reaction, the indicated substrate (Rho-S(Ub)G, Rho-T(Ub)G, or Tamra-K(Ub)G) was present at 50 nM. For DUB panels, 0.5 μM of each DUB was used. To find the optimal concentration of $TssM^{Bp}$ ($TssM^{Bp\Delta N191}$) for each substrate, a series of dilutions were prepared and FP was measured. The optimal concentration of $TssM^{Bp}$ was 0.4 nM for ester-linked substrates and 4 nM for the isopeptide-linked substrate. These concentrations were then used to monitor activity of the indicated point mutants. All working solutions were prepared by diluting enzyme stocks into the FP buffer (25 mM HEPES (pH 7.4), 150 mM NaCl, 0.1 mg/mL BSA, 5 mM β-mercaptoethanol).

To collect data, a 2X stock of substrate (i.e., 100 nM) was added to the microplate and monitored for 5 min to establish a baseline FP (∼177 mP). The plate was removed from the plate reader and a 2X stock of DUB was added 1:1 to establish the final reaction conditions. All reactions were performed in triplicate, and data were processed following blank subtraction. Graphs depicting WT $TssM^{Bp}$ against $TssM^{Bp}$ mutants show representative datasets that were collected simultaneously. For dilution experiments used to determine the catalytic efficiency of vOTU, JOSD1, $TssM^{Bp}$, V466R $TssM^{Bp}$, or $TssM^{Cs}$, the FP data corresponding to substrate cleavage was analyzed by non-linear regression using a one-phase decay fit from GraphPad Prism 9. Here, the Y_0 was set to the average mP of each substrate prior to DUB addition (∼177 mP), and the plateau was set to the average mP of the cleaved fluorescent peptide (∼50–60 mP). For each substrate and DUB combination, the plateau was calculated from the highest concentration of DUB tested to ensure the mP value reflected a reaction that had gone to completion. Rate constants (k) were determined for each concentration by constraining k to be shared between all replicates ($n = 3$). Rate constants and the associated standard error of the mean (SEM) were extracted and graphed against the concentration of DUB. Repeating this processing over a range of concentrations yielded linear fits that corresponded to the k_{cat}/K_M (in $M^{-1}s^{-1}$; catalytic efficiency).

Protein expression and purification

E. coli Rosetta cells carrying pETM30-His-GST-$TssM^{Bp\Delta N191}$ and its variants were grown at 37°C until OD_{600} reached 0.6, and protein expression was induced with the addition of 0.5 mM IPTG at 16°C overnight. Cells were harvested and pellets were resuspended in 25 mM Tris-HCl (pH 7.5), 500 mM NaCl, 10 mM imidazole, 10% glycerol and lysed on ice by sonication. Lysates were clarified by centrifugation at 45,000 × *g* for 1 h, and the supernatant was applied to Ni-NTA resin for affinity purification. After binding, the resin was washed with 25 mM Tris-HCl (pH 7.5), 500 mM NaCl, 35 mM imidazole, 10% glycerol. His-GST-$TssM^{Bp\Delta N191}$ proteins were eluted using 25 mM Tris (pH 7.5), 250 mM NaCl, 250 mM imidazole, 10% glycerol. The His-GST tag was removed from the TssM proteins by incubating with Tobacco Etch Virus (TEV) protease for 4 h at room temperature. While cleaving, protein mixtures were dialyzed against 4 L of 25 mM Tris-HCl (pH 7.5), 250 mM NaCl, 5% glycerol to remove imidazole. After 4 h, the solution was purified further using Ni-NTA resin pre-washed with dialysis buffer. The flowthrough was collected and concentrated for size exclusion chromatography using a Superdex 200 16/600 gel filtration column pre-equilibrated in 25 mM Tris-HCl (pH 7.4), 150 mM NaCl, 2 mM β-mercaptoethanol.

His-3C-$TssM^{Cs}$ (59–347) was expressed from the pOPINB vector using the same induction protocol as His-GST-$TssM^{Bp\Delta N191}$. Purification of $TssM^{Cs}$ was as for His-GST-$TssM^{Bp\Delta N191}$ with the exception of His-tag removal by 3C protease instead of TEV. All other details including buffers and columns were the same.

His-tagged human JOSD1 was expressed from a pET28b vector (kind gift from S. Buhrlage) in *E. coli* Rosetta cells. Protein expression was induced at OD_{600} of 0.6 using 0.5 mM IPTG overnight at 16°C. The cells were harvested, resuspended, lysed and initially purified as described above for TssM. Once eluted off the Ni-NTA resin, the protein solution was concentrated for size exclusion chromatography using the same buffer as $TssM^{Bp\Delta N191}$.

For all proteins, protein purity was confirmed by SDS-PAGE before fractions were concentrated, quantified by absorbance, and flash frozen for storage at −80°C. All other DUBs used in this study were purified as described previously: RickCE 378–691, SseL 24–340, ShiCE 2–405[37]; SpvD R161G full length[36]; Crimean-Congo Haemorrhagic Fever Virus vOTU 1–185[31]; LotA full length,[38] ChlaDUB1 130–401 and ChlaDUB2 80–339.[52]

SDS-PAGE and immunoblotting

Samples, prepared in a Laemmli buffer containing 5% β-mercaptoethanol, were boiled for 5 min prior to protein separation by SDS–PAGE using either 10% or 15% Tris polyacrylamide gels. Following transfer to PVDF membrane (Millipore) and blocking overnight in 5% milk (or BSA) in PBS-Tween, the membranes were incubated with the indicated primary antibodies. HRP-conjugated secondary antibodies (Dako) were used for detection using ECL detection reagents (Cytivia ECL and Pierce ECL2) on a Chemidoc Touch Imaging System (Bio-Rad).

Synthesis of ester-linked substrates

To generate Rho-S(Ub)G and Rho-T(Ub)G substrates, C-terminal *tert*-butyl protected dipeptides H-Ser-Gly-OtBu and H-Thr-Gly-OtBu were made using standard peptide coupling conditions. *N*,*N*′-diBoc-5-carboxy-Rhodamine[53] was coupled to the N-terminus of both peptides, followed by esterification of the Ser and Thr sidechain OH with FmocGlyOH using EDC and HOBt. The Fmoc protecting group was removed from the Gly amine, which was subsequently coupled to fully protected Ub 1–75 with a free C-terminal carboxylic acid (prepared by solid-phase peptide synthesis[54]). Global deprotection was achieved with 90% TFA and the resulting ester-linked ubiquitin FP reagents were purified by RP-HPLC. Detailed methods are available in the Supplemental Information (Methods S1).

TssM crystallization and structure analysis

TssM ($TssM^{Bp\Delta N191}$) protein for crystallographic studies was prepared as described above, with minor changes. Following purification on Ni-NTA resin, the protein was further purified on glutathione resin prior to on-column cleavage with TEV. Ni-NTA resin was used to capture TEV protease from the eluted TssM prior to concentration and final purification by size exclusion chromatography on a Superdex 75 16/600 column. Ub-Propargylamide (PA) activity-based probe was prepared as previously described using intein chemistry.[29,38,55] TssM was reacted with Ub-PA at a 1:2 M ratio overnight on a roller at room temperature in the presence of fresh 5 mM DTT. The reaction was purified by sequential rounds of ion exchange using a HiTrap Q HP column. The first round was performed in 25 mM Tris (pH 7.0), 50 mM NaCl with an elution gradient to 1 M NaCl. The TssM-Ub complex was present primarily in the flowthrough and early elution fractions, which were pooled and run over the column again at pH 8.0. The resulting TssM-Ub product was dialyzed against 20 mM Tris (pH 8.0), 150 mM NaCl and concentrated to 15 mg/mL for crystallography studies. Crystals were obtained in sitting drop format using a 100 nL drop comprised of 15 mg/mL TssM-Ub combined 1:1 with reservoir solution containing 1.4 M Sodium phosphate monobasic monohydrate/Potassium phosphate dibasic pH 5.6. Crystal trays were stored at room temperature, where crystals grew within two weeks. The resulting crystals were cryoprotected in mother liquor containing 30% glycerol prior to vitrification.

Diffraction data were collected at Diamond Light Source, Beamline I24, with a wavelength of 0.999903 Å and temperature of 100 K. The data were integrated using Dials[56] and scaled with Aimless.[57] Molecular replacement was performed with the Phaser module of CCP4i2 using an AlphaFold model of the TssM USP domain and a previously determined structure of Ub.[46,58–60] Automated model building of the Big5 domain was performed using Buccaneer,[61] followed by iterative manual building in Coot and refinement in PHENIX.[62,63] Final Ramachandran statistics: 96.36% favored, 3.49% allowed, 0.15% outliers. All structure figures were produced using PyMol (www.pymol.org).

Ubiquitylated maltoheptaose assay

Ubiquitylated maltoheptaose was prepared as previously described.[35] A loading reaction containing 0.5 μM UBE1, 1.5 μM UBE2L3, 1.8 μM HOIL-1, 30 μM ubiquitin, 1.8 μM K63-linked di-ubiquitin, 20 mM maltoheptaose, 5 mM $MgCl_2$, and 5 mM ATP was incubated at 37°C for 2 h, after which the loading was quenched with 20 mM DTT and 20 mM EDTA. The quenched loading reaction was then divided and treated with 70 mM DTT, 70 mM NaOH, 0.5 μM vOTU, 0.5 μM $TssM^{Bp}$, or 0.5 μM $TssM^{Bp}$ V466R for 1 h at 37°C. Reactions were then quenched in SDS sample buffer and analyzed by SDS-PAGE for abundance of di-ubiquitin and ubiquitylated maltoheptaose.

QUANTIFICATION AND STATISTICAL ANALYSIS

Data were tested for statistical significance with GraphPad Prism software. The number of replicates for each experiment and the statistical test performed are indicated in the figure legends. Significance was defined as $*p < 0.05$; $**p < 0.01$; $***p < 0.001$; **** <0.0001.